Ocean Dynamics (2005) 55: 178–198
DOI 10.1007/s10236-005-0006-5

J. Eric Jones · Alan M. Davies

# An intercomparison between finite difference and finite element (TELEMAC) approaches to modelling west coast of Britain tides

Published online: 27 August 2005


**Abstract** A finite element model (namely TELEMAC) with a range of mesh refinements and assumptions of coastal water depths is used to determine an optimal mesh for computing the $M_2$ tide in a region of significant geographical extent. The region adopted is the west coast of Britain covering the Irish and Celtic Seas. The nature of the spatially varying topography and tidal distribution, together with a comprehensive set of measurements and existing accurate finite difference model makes it ideal for such a study. Calculations show that a water-depth dependent criterion for determining element size gives an optimal distribution over the majority of the region. However, local refinements in narrow channels such as the North Channel and Bristol Channel are required. Although the specification of a zero coastal water depth, leads to a fine near coastal grid, this does not yield the most accurate solution. In addition the computational cost is high. In practice in a large area model the use of a non-zero coastal water depth yields optimum accuracy at minimal computational cost. However, calculations show that accuracy is critically dependent upon nearshore water depths. Comparison with the finite difference model shows that the bias in elevation amplitude in the finite difference solution is removed in the finite element calculation.

## Introduction

Recent storm surge modelling on the west coast of Britain using a finite difference grid (Fig. 1) (e.g. Jones and Davies 2004a, b), Davies et al. 2001a) has shown the need to use a large area model in order to account for 'far field' wind effects. These are a major contribution, in many cases more important than the local wind induced surge, in determining the storm surge elevation at the coast. In a uniform grid finite difference model, the approach has been to use a coarse grid large area model to provide boundary conditions for a local area finer grid model (e.g. Davies et al. 2001b; Jones and Davies 1998; Davies and Hall 2002). By this means the grid is refined in the region where high resolution is required without the computational overhead of using a fine resolution everywhere. One major problem with this approach is the abrupt change in grid resolution from one area to another and the need to use an appropriate boundary condition along the open boundary of the higher resolution model. Difficulties have recently been shown (Jones and Davies 2004a, b, Davies and Hall 2002) with formulating an open boundary condition which is suitable for a range of locations (e.g. shelf edge to shallow sea) and types of surges (e.g. positive and negative surges). This suggests that a graded grid with the ability to refine it locally, such as that provided by finite elements is desirable. Although the finite element method is a good means of producing a local grid refinement, it is not the only approach. A comprehensive review of the range of methods that are available for grid refinement and the advantages/disadvantages of each is given in Jones (2002).

In order to achieve an accurate storm surge prediction on the west coast of Britain it is essential to include an accurate description of the tides within the model. This is necessary because tidal currents are important in determining the background level of friction in the region and cannot be readily linearized as they exhibit significant spatial variability in the area. Tide-surge interaction is also important in shallow water. Consequently before proceeding to produce a finite element surge model of the region, it is essential to develop an accurate finite element tidal model. To this end, an optimal choice of graded mesh, through careful local refinement of the mesh (Table. 1, 2) is essential in determining an accurate solution in near coastal regions

Responsible Editor: Phil Dyke

J. E. Jones (✉) · A. M. Davies
6 Brownlow Street,
Liverpool, L3 5DA, UK
E-mail: jej@pol.ac.uk

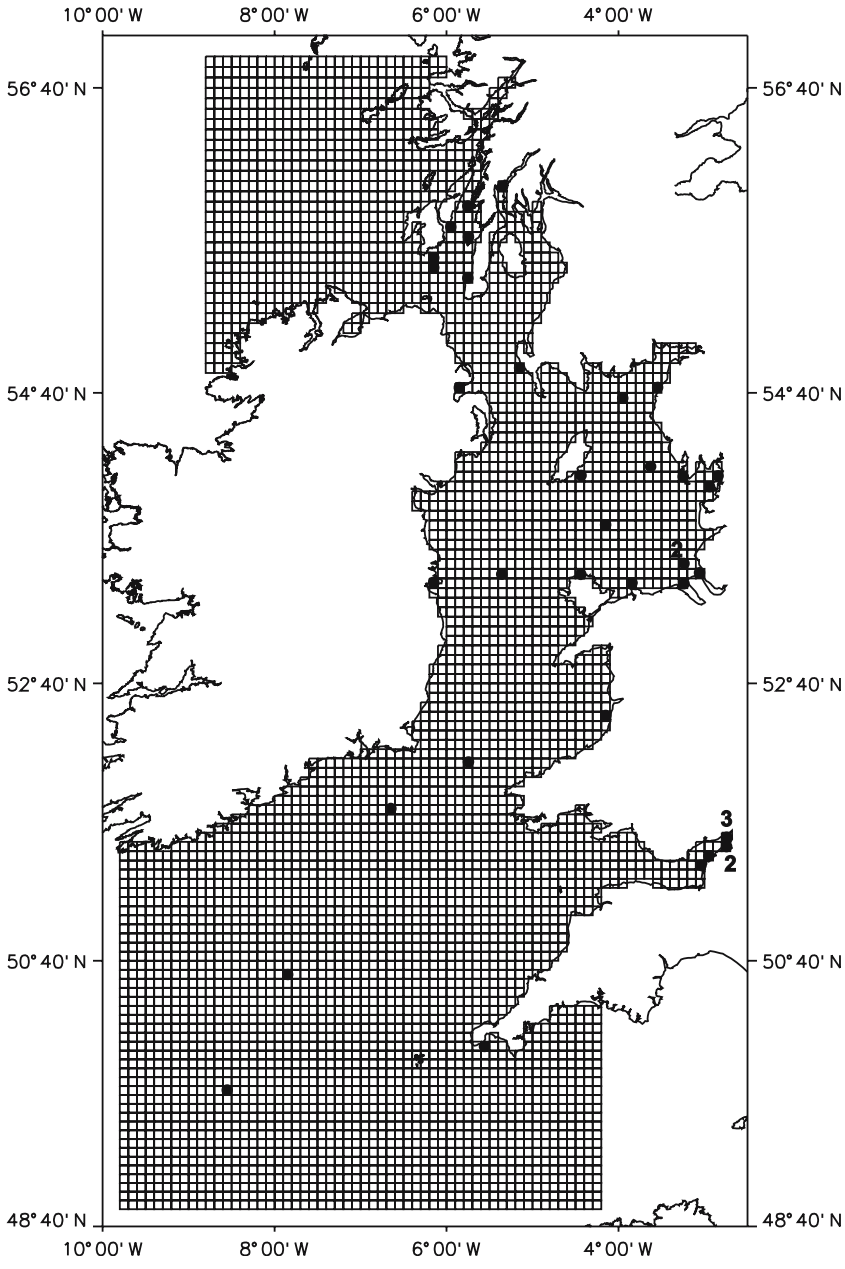


**Fig. 1** Finite difference grid of the west coastal model. Also marked are the locations of ports used in the detailed comparison tables

**Table 1** Summary of Calculations

| Calc | Grid |
|---|---|
| BM | Uniform finite difference grid of about 7 km resolution |
| 1 | G0: uniform finite element of about 7 km resolution |
| 2 | G1: as G0, but refined in North Channel and Bristol Channel |
| 3 | G2: number of element of same order as G0, but refined in near coastal regions using $(gh)^{1/2}$ |
| 4 | G3: refined grid using topography related to bathymetry as in G2, but eastern Irish Sea topography from 1 km model of Jones and Davies (1996) |
| 5 | G4: as grid G3, but with enhanced resolution in the Mersey estuary |
| 6 | G5: as grid G3, but with enhanced resolution in the Bristol Channel |
| 7 | G0X: as G0 but with non-zero water depths along the coast |
| 8 | G2X: as G2, but with non-zero water depths along the coast |
| 9 | G3X: as G3 but with non-zero water depths along the coast |
| 10 | G3XB: as G3X but with higher order element |

**Table 2** Summary of number of nodes and run times

| Calc | Grid | Characteristic nodes, elements, run times | | |
|---|---|---|---|---|
| | | Nodes | Elements | Run times |
| 1 | G0 | 11,828 | 22,409 | 12 h 12 m |
| 2 | G1 | 12,212 | 23,119 | 14 h 14 m |
| 3 | G2 | 10,442 | 18,769 | 08 h 39 m |
| 4 | G3 | 11,702 | 21,018 | 10 h 02 m |
| 5 | G4 | 12,334 | 22,221 | 11 h 38 m |
| 6 | G5 | 11,112 | 19,991 | 10 h 17 m |
| 7 | G0X | 11,828 | 22,409 | 02 h 11 m |
| 8 | G2X | 5,320 | 9,604 | 00 h 45 m |
| 9 | G3X | 6,842 | 12,265 | 01 h 36 m |
| 10 | G3XB | 6,842 | 12,265 | 02 h 33 m |

*Note* G3XB uses a higher order element

(e.g. Liverpool Bay) (Fig. 2) and channels (e.g. the Bristol Channel). To what extent refining the mesh in offshore regions to improve the location of tidal amphidromes (often used in finite difference models as an indication of model's accuracy) is useful when high accuracy is needed in coastal regions, is also considered here. In addition the extent to which refinement in regions such as the North Channel (Fig. 2) influences the dynamics of the eastern Irish Sea is also examined.

The primary objective of the paper is to develop an accurate two-dimensional finite element tidal model of the west coast of Britain that can subsequently be used in storm surge simulations and extended to three-dimensional circulation problems. An important part of this development at an early stage involves examining the sensitivity of the global solution to grid refinement in specific regions. By this means a cost effective optimal distribution of elements can be achieved. This is essential before proceeding to three-dimensional and a multi-tidal constituent storm surge model. The region covered by the model (Fig. 1) is identical to that used previously with a coarse grid (about 7 km resolution) finite difference model. This area is chosen because accurate tidal open boundary conditions are available. In addition there are tidal solutions from a 7-km finite difference grid that can be used as a 'bench mark' solution. By using the same topography as in this model, differences due to varying the grid and assumptions of coastal water depths can be examined.

Although a general finite difference/finite element comparative study of tides was made in the English Channel as part of the Tidal Flow Forum (see Werner 1995 for a review of the results) a comparable exercise has never been performed over a large region such as the west coast of Britain. Also in this paper we look at the effect of various means of refining the grid upon both the global and local solution, which was never examined in detail in the Tidal Flow Forum. Also, the rapid spatial variability of the tides in regions such as the North Channel, Liverpool Bay and Bristol Channel adds a degree of complexity not found in the English Channel. In addition the use of a zero or non-zero water depth at the coast upon the degree of 'wetting and drying' and how this influences the accuracy of the solution, and the computational time has not been examined previously. Although the influence of grid resolution and refining topography upon the convergence of a large area barotropic tidal model has been examined (Luettich and Westerink 1995) no comparable near coastal study in the form presented here has been performed. To date some limited irregular grid modelling has been performed off the west coast of Britain using a map projection method to give a finer grid in the North Channel (Young et al. 2000, 2001). Although this approach can enhance the grid in one specific area, it cannot resolve the near coastal region as in the finite element meshes used here.

The form of the hydrodynamic equations is outlined in the next section. Their numerical solution using a regular finite difference grid or finite element approach using the TELEMAC code is presented subsequently. Later sections deal with the development of a 'base line' solution using a regular finite element grid of comparable resolution to the finite difference grid. Comparison with this 'base line' solution can be used to determine how re-distribution of elements leads to a local improvement or degradation of the solution as the grid in one area is refined at the expense of a coarser grid elsewhere. In these calculations the number of elements remained approximately constant. Subsequently the effect of a local enhancement in which the number of grid elements is increased in a specific region is examined. The computational overhead as a function of the increased number of elements is examined in this case.

The use of various criteria to refine the mesh, in particular mesh size dependent on water depth is considered in terms of model's accuracy. In connection with this the application of a zero water depth at the coast, leading to fine nearshore elements, or a finite coastal depth leading to coarser nearshore elements is examined. The implications of a zero or non-zero coastal water depth in terms of 'wetting and drying' at low water are also considered. The application of higher order elements is also briefly investigated. Conclusions as to the accuracy of a finite element model of tides in the region and the effects of local grid refinement are given in the final section of the paper.

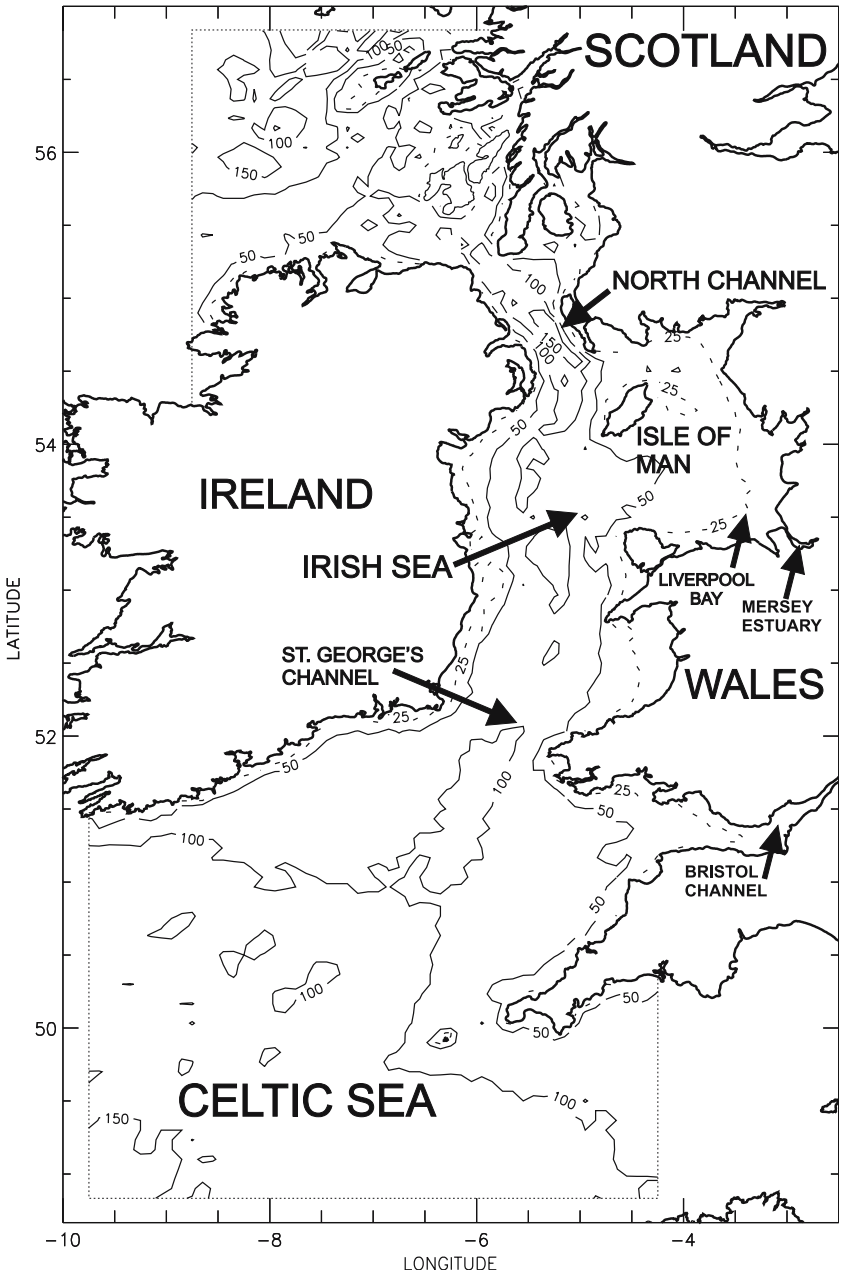


**Fig. 2** Locations named in the text, and water depth distribution in the region

## Fundamental equations and form of models

### Basic equations

Since the aim of the paper is a study of the sensitivity of the tidal distribution to variations in horizontal grid resolution, then the solution of the two-dimensional vertically integrated hydrodynamic equations is sufficient. As the region spans a range of latitude, the hydrodynamic equations in spherical coordinates were solved, using both a finite difference and finite element approach.

These are given by

$$\frac{\partial \zeta}{\partial t} + \frac{1}{R\cos\phi}\frac{\partial}{\partial \phi} V\cos\phi + \frac{1}{R\cos\phi}\frac{\partial}{\partial \chi} U = 0 \tag{1}$$

$$\frac{\partial U}{\partial t} + S_u - 2\omega\sin\phi\, V = \frac{-g}{R\cos\phi}\frac{\partial \zeta}{\partial \chi} + \frac{\tau_\chi}{\rho(h+\zeta)} \tag{2}$$

$$\frac{\partial V}{\partial t} + S_v + 2\omega\sin\phi\, U = \frac{-g}{R}\frac{\partial \zeta}{\partial \phi} + \frac{\tau_\phi}{\rho(h+\zeta)} \tag{3}$$

where $S_u$, $S_v$ are the non-linear momentum terms, details of which are given in Davies and Jones (1992).

The nomenclature in these equations is $\chi$, $\phi$, east longitude, (positive eastward) and north latitude (positive northward), respectively, $h$ depth below the undisturbed depth of water, $t$ time, $\zeta$ elevation of the sea surface above the undisturbed level, $\rho$ the density of sea water, $R$ the radius of the Earth, $\omega$ the angular speed of the Earth's rotation, g the acceleration due to gravity, $U$, $V$ eastward and northward components of current, $\tau_\chi$, $\tau_\phi$ components of bottom stress given by

$$\tau_\chi = k\rho U\left(U^2 + V^2\right)^{1/2}, \quad \tau_\varphi = k\rho V\left(U^2 + V^2\right)^{1/2} \tag{4}$$

with $k$ a coefficient of bottom friction. In the calculations this was fixed at $k = 0.0025$, an appropriate value to use in a two-dimensional model and consistent with Davies and Jones (1992).

### Initial and boundary conditions

All solutions were generated from initial conditions of zero elevation and motion at $t = 0$. At a closed boundary the normal component of velocity was set to zero. The horizontal gradient normal to the coast of alongshore velocity was taken as zero, corresponding to perfect slip. In shallow water areas at times of low tide regions can dry with subsequent wetting later in the tidal cycle. A description of this in terms of methods used in finite difference models is given in Flather and Hubbert (1989). In the TELEMAC code a range of options is possible including removing all elements which are not wet from the solution, in essence adjusting the grid in the nearshore region with the associated computational overhead. In these calculations this was not done but the terms in the hydrodynamic equations which became physically unrealistic were removed from the solution. This is consistent with methods used in finite difference models where the grid did not change (Flather and Hubbert 1989). In the finite element model in shallow water regions where significant 'wetting and drying' occurs energy is lost to higher harmonics and this influences the $M_2$ tidal distribution. This will be discussed in more detail later in the paper.

Along the open boundaries the $M_2$ tidal elevation was specified. The input was identical to that used by Davies and Jones (1992) in their three-dimensional multi-constituent calculation. In all computations the same tidal input was used. In the finite element calculations in which the grid was refined to give enhanced resolution in near coastal regions with coarser resolution offshore, the tidal input was interpolated to the new open boundary nodes. Solutions were determined in all cases by integrating forward in time over seven tidal cycles and harmonically analysing the final cycle to yield tidal amplitude and phase.

A preliminary calculation showed that although TELEMAC iterated at each time step to ensure convergence, it was necessary to integrate in time for a sufficiently long period for the tide to propagate several times through the domain. This was necessary to allow frictional dissipation in shallow coastal regions to influence the offshore distribution of the tide. A shorter period integration would be required in a limited area nearshore region where TELEMAC is usually applied (Hervouet 2002).

## Finite difference 'bench mark' (BM) solution

In order to compare the accuracy of the finite element model using a range of grid refinements, with solutions derived with the finite difference model it is necessary to generate a 'bench mark' finite difference solution. To this end the uniform finite difference three dimensional multi-tidal constituent model of Davies and Jones (1992) was run in two-dimensional form for just the $M_2$ tide. The $M_2$ tidal input and water depths were identical to those used previously (Davies and Jones 1992). The grid resolution of the model is 4' north-south by 6' west-east (about 7 km) and covers the region shown in Fig. 1. The topography of the area is characterized by deep water ($h = 100$ m) areas in the region to the west of Scotland (Fig. 2) and in the Celtic Sea. In the eastern Irish Sea water depths reach the order of 50 m in the deep areas, with nearshore regions that in a high resolution (of order 1 km) model (Jones and Davies 1996), exhibit 'wetting and drying' over a tidal cycle. The Bristol Channel region has a large tidal range ($M_2$ tidal amplitude of order 4.2 m) with associated 'wetting and drying'.

The $M_2$ cotidal chart (Fig. 3) computed with the two-dimensional finite difference model (Table 1, Calc BM) is comparable to that derived by Davies and Jones (1992) using a three-dimensional model with identical grid resolution. The objective in presenting it here is to show in essence a 'benchmark solution' with which finite element solutions can be compared. Comparison with this and with tide gauges results (location of tide gauges given in Table 3) presented in Table. 4, 5, 6 as the finite element grid is refined and is discussed later. The spatial distribution of co-amplitude and co-phase lines (Fig. 3) are in good agreement with cotidal charts of the region based on observations (Robinson 1979; Howarth 1990), showing a degenerate amphidrome off the east coast of Ireland and in the North Channel (Fig. 3). Tidal amplitudes increase rapidly in Liverpool Bay and the Bristol Channel as water depths decrease.

To quantify the differences between the various models and observations a comprehensive data set of 214 observations of the $M_2$ tide based on coast and offshore gauges was used. To date this is the most comprehensive data set available in the region. A selection of results in various regions of the model (see Table 3, for port locations) is presented in Table 4 in order to illustrate the effects of various grid resolution

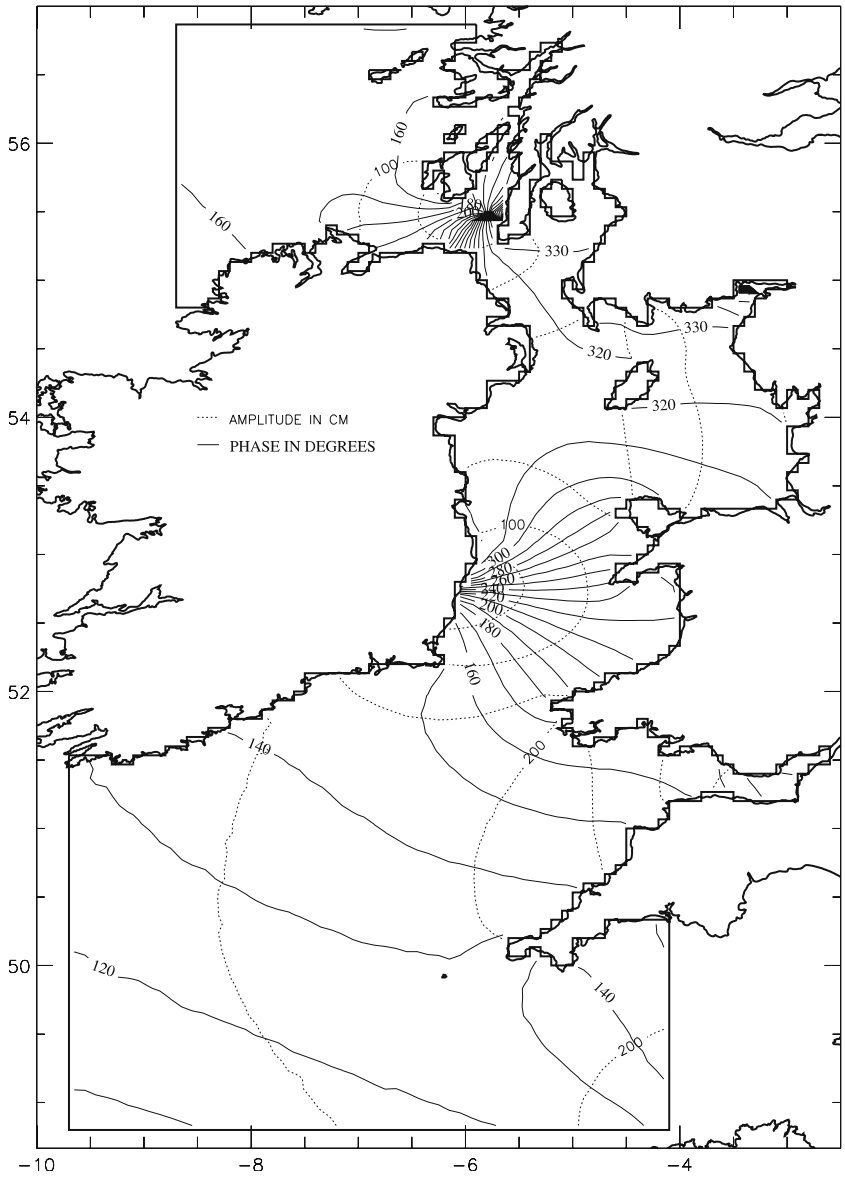


**Fig. 3** Computed $M_2$ cotidal chart (dashed line amplitude (cms)), solid line phase in degrees

changes. The influence of grid resolution upon water depth at comparison points is given in Table 5. A global estimate of model's accuracy based on all 214 observations is summarized by the histogram of errors given in Table 6. Also presented are standard deviation and root mean square (RMS) errors in amplitude and phase. This comparison of errors in consistent with that used by Jones and Davies (1996) (see also results in Jones 1983).

An overall measure of the model's performance $H_S$, which takes into account differences in both amplitude and phase between model and observations, computed from

$$H_S = \left\{ (H_1)^2 + (H_2)^2 \right\}^{1/2}$$

with

$$H_1 = H_o \cos(g_o) - H_c \cos(g_c)$$

$$H_2 = H_o \sin(g_o) - H_c \sin(g_c)$$

is also given. In these equations $H_o$, $g_o$, $H_c$, $g_c$ denote amplitude and phase of observed and computed $M_2$ tidal amplitude. An average value of $H_S$, namely $\bar{H}_S$ determined by summing over all ports and dividing by the number of ports is given in Table 4. Also presented are $H_{EX}$ and $\bar{H}_{EX}$, which are comparable to $H_S$ and $\bar{H}_S$ but computed with a limited number of ports. In determining $H_{EX}$ and $\bar{H}_{EX}$, locations in the North Channel and Bristol Channel where the model's grid cannot resolve the region and hence the rapid phase change are excluded. Similarly deviations and RMS errors based upon the omission of these regions is presented (Table 6).

The physical characteristic of the tide in the Irish Sea, is that it enters through both the North Channel and Celtic Sea regions, giving rise to a standing wave. Consequently, in order to obtain the correct representation

**Table 3** Latitude and longitude of various locations used in comparison tables

| No. | Port | Latitude (N) | Longitude (W) |
|---|---|---|---|
| 4 | Aberystwyth | 52.41667 | 4.09167 |
| 7 | Ardminish Bay | 55.68333 | 5.73333 |
| 11 | Aust | 51.60000 | 2.63333 |
| 12 | Avonmouth | 51.51025 | 2.71408 |
| 20 | Barrow | 54.06667 | 3.16667 |
| 25 | Beachley | 51.61666 | 2.65000 |
| 27 | Belfast | 54.60472 | 5.92111 |
| 43 | B | 51.75000 | 6.60000 |
| 48 | F | 50.55000 | 7.53333 |
| 51 | G | 49.66667 | 8.53333 |
| 56 | Clevedon | 51.45000 | 2.85000 |
| 64 | Craighouse | 55.83333 | 5.95000 |
| 71 | Douglas | 54.14611 | 4.46667 |
| 72 | Dublin | 53.35000 | 6.21667 |
| 89 | Heysham | 54.03333 | 2.91667 |
| 90 | Hilbre Island | 53.38334 | 3.21667 |
| 98 | Inward Rocks | 51.65000 | 2.61667 |
| 100 | Islay | 55.62756 | 6.18892 |
| 108 | Liverpool | 53.44942 | 3.01667 |
| 110 | Liverpool Bay | 53.48333 | 3.25000 |
| 112 | Llandudno | 53.33150 | 3.82367 |
| 114 | Loch Inver | 56.15000 | 5.25000 |
| 119 | Macrahanish | 55.43333 | 5.75000 |
| 128 | Morecambe | 54.08333 | 2.88333 |
| 133 | Newlyn | 50.10233 | 5.54183 |
| 137 | OSTG-G(Q) | 53.50000 | 3.21667 |
| 138 | OD | 53.43333 | 5.36667 |
| 139 | ON | 52.06667 | 5.78333 |
| 153 | Bristol | 51.50000 | 2.71667 |
| 163 | Portpatrick | 54.84241 | 5.11889 |
| 191 | STD(S) | 53.76667 | 4.11667 |
| 195 | Stn D | 55.86666 | 5.73333 |
| 196 | Stn E | 55.46667 | 6.16667 |
| 198 | STN34 (U) | 54.15000 | 3.66667 |
| 199 | STN35 (V) | 54.65000 | 3.91667 |
| 210 | Weston-s-Mare | 51.35000 | 2.98333 |
| 213 | Workington | 54.65000 | 3.56667 |
| 214 | Wylfa Head | 53.41667 | 4.46667 |

of the tides in the eastern Irish Sea, it is essential to correctly reproduce the tidal propagation in the North Channel and Celtic Sea regions (Table 4).

It is evident from Table 4 that the tidal amplitude in the North Channel is accurately reproduced in the BM model, although there are some errors in phase suggesting that the amphidromic point is not in its correct location. Recent calculations with a high resolution (of order 1 km) limited area model (Davies et al. 2001b) have shown the importance of using a fine grid in this region. The influence of enhancing local resolution will be examined in connection with the finite element model.

In the Celtic Sea area it is apparent that on average at offshore tide gauges OD, ON, B, F and G (approximate locations shown in Fig. 1, with exact positions in Table 3) the model has a slight bias to overpredict the amplitude with reasonable agreement in phase particularly at B, F, G (Table 4). Within the deep water parts of the Irish Sea (neglecting the eastern Irish Sea), the amplitude is in reasonable agreement with observations (Table 4).

In the Bristol Channel region, there is reasonable agreement (see Table 4) with the observed amplitude, although the phase is on average too high. This agreement is rather surprising since the resolution in this region is rather poor. The accuracy of the model in this area probably reflects the fact that depths in the finite difference grid box, are not point values, but a grid box average, designed to give the correct cross-sectional volume transport. In the finite difference model each grid box has a fixed depth over the total extent of the box, even when the box is adjacent to a coast, which is represented as a vertical wall. In the initial calculations (Calcs 1–6, Table 1) with the finite element model a linear decrease to zero is assumed as the coast is approached. Consequently, in the finite element model in the coastal region the average depth is reduced. The consequences of this will be examined in the finite element calculations. However, in subsequent calculations (Calcs 7–10, Table 1) a non-zero coastal water depth was assumed. How this influences the finite element solution compared with the use of a zero water depth will be considered later in the paper.

Amplitudes and phases at offshore tide gauges in the eastern Irish Sea determined with the finite difference model (Table 4) on average showed good agreement with observations, suggesting that the tidal wave entering the eastern Irish Sea was correctly reproduced in the model. However, on average at coastal gauges in the eastern Irish Sea, the model tended to underestimate the tidal amplitude. This is probably because of a lack of resolution in the region, since Jones and Davies (1996) using a three-dimensional model with a 1-km grid found an improvement in accuracy in the area.

Despite the coarse grid nature of the model, based on all tide gauges the average deviation in amplitude and phase was 6.02 cm and $-1.45°$ with RMS errors of 16.9 cm and 20°. The overall error $\bar{H}_S$ was 33.6 cm (Table 6). Values of $\bar{H}_R$ and RMS errors based upon the set of locations excluding the North Channel and Bristol Channel are significantly reduced, (in particular the RMS error in phase) below the corresponding values from the full set of points. Although this suggests a reasonably accurate solution, it is evident from Table 6, that there is a significant bias to overpredict amplitudes and underpredict phases. This suggests a fundamental error in the solution possibly resulting from the application of a coarse grid.

## Finite element calculations

### Topography based on the west coast model

To examine to what extent using a finite element code (namely TELEMAC) changes the computed tidal distribution, the previous calculation was repeated (Calc 1, Table 1). To provide a baseline from which changes in mesh resolution could be judged, a uniform finite element grid (GO) was generated (Fig. 4). This grid has

**Table 4** Comparison of observed and computed amplitude $h$ (cm) and phase $g$ (deg) for various ports

| Port | Obs | | BM | | Calc 1 | | Calc 2 | | Calc 3 | | Calc 4 | | Calc 5 | | Calc 6 | | Calc 7 | | Calc 8 | | Calc 9 | | Calc 10 | |
|---|---|---|---|---|---|---|---|---|---|---|---|---|---|---|---|---|---|---|---|---|---|---|---|---|
| | $h$ | $g$ | $h$ | $g$ | $h$ | $g$ | $h$ | $g$ | $h$ | $g$ | $h$ | $g$ | $h$ | $g$ | $h$ | $g$ | $h$ | $g$ | $h$ | $g$ | $h$ | $g$ | $h$ | $g$ |
| Eastern Irish Sea | | | | | | | | | | | | | | | | | | | | | | | | |
| 20 Barrow | 292 | 327 | 280 | 323 | 308 | 314 | 318 | 315 | 307 | 316 | 312 | 319 | 277 | 324 | 279 | 323 | 313 | 313 | 325 | 316 | 324 | 321 | 321 | 323 |
| 71 Douglas | 231 | 327 | 215 | 322 | 237 | 312 | 228 | 312 | 225 | 312 | 238 | 313 | 236 | 313 | 241 | 315 | 246 | 313 | 237 | 313 | 243 | 312 | 240 | 313 |
| 89 Heysham | 316 | 326 | 306 | 330 | 322 | 318 | 327 | 317 | 320 | 318 | 322 | 315 | 320 | 314 | 322 | 316 | 337 | 317 | 335 | 317 | 335 | 317 | 333 | 318 |
| 90 Hilbre | 292 | 318 | 286 | 312 | 304 | 303 | 308 | 303 | 303 | 303 | 313 | 305 | 304 | 309 | 309 | 307 | 321 | 305 | 318 | 304 | 330 | 306 | 325 | 307 |
| 108 Liverpool | 304 | 321 | 292 | 313 | 314 | 306 | 316 | 306 | 310 | 305 | 305 | 308 | 96 | 299 | 308 | 309 | 323 | 305 | 322 | 305 | 323 | 311 | 321 | 311 |
| 110 Liverpool Bay | 262 | 315 | 284 | 313 | 303 | 303 | 305 | 304 | 302 | 304 | 303 | 304 | 303 | 304 | 305 | 305 | 318 | 305 | 317 | 305 | 321 | 305 | 318 | 306 |
| 128 Morecambe | 308 | 326 | 315 | 340 | 325 | 319 | 323 | 327 | 309 | 334 | 267 | 322 | 293 | 322 | 231 | 327 | 343 | 320 | 341 | 319 | 297 | 300 | 293 | 327 |
| 213 Workington | 274 | 333 | 265 | 341 | 293 | 329 | 291 | 317 | 283 | 328 | 279 | 316 | 280 | 317 | 284 | 319 | 300 | 325 | 293 | 319 | 292 | 318 | 289 | 318 |
| 214 Wylfa Head | 207 | 300 | 208 | 298 | 225 | 290 | 229 | 291 | 223 | 290 | 221 | 290 | 218 | 290 | 227 | 291 | 235 | 292 | 227 | 291 | 230 | 291 | 228 | 291 |
| 112 Llandudno | 268 | 310 | 255 | 306 | 278 | 298 | 279 | 298 | 277 | 299 | 280 | 299 | 279 | 298 | 281 | 299 | 291 | 300 | 291 | 300 | 297 | 300 | 293 | 300 |
| Eastern Irish Sea off-shore gauges | | | | | | | | | | | | | | | | | | | | | | | | |
| 137 OSTG-G (Q) | 290 | 316 | 284 | 313 | 302 | 304 | 307 | 304 | 302 | 304 | 304 | 304 | 303 | 306 | 306 | 305 | 317 | 305 | 317 | 305 | 322 | 306 | 319 | 306 |
| 191 STD (S) | 236 | 317 | 228 | 312 | 248 | 303 | 249 | 305 | 246 | 304 | 247 | 306 | 248 | 304 | 248 | 303 | 259 | 304 | 256 | 305 | 263 | 305 | 260 | 305 |
| 198 STN34 (U) | 264 | 325 | 261 | 323 | 276 | 311 | 280 | 311 | 273 | 312 | 272 | 311 | 273 | 311 | 274 | 311 | 287 | 312 | 284 | 313 | 288 | 312 | 284 | 312 |
| 199 STN35 (V) | 256 | 333 | 250 | 331 | 270 | 318 | 271 | 319 | 266 | 319 | 266 | 317 | 265 | 317 | 269 | 318 | 277 | 320 | 276 | 321 | 279 | 319 | 276 | 319 |
| Irish Sea/Celtic Sea | | | | | | | | | | | | | | | | | | | | | | | | |
| 27 Belfast | 120 | 316 | 126 | 313 | 154 | 310 | 152 | 307 | 152 | 309 | 154 | 310 | 154 | 311 | 155 | 310 | 144 | 303 | 144 | 303 | 149 | 304 | 149 | 305 |
| 163 Portpatrick | 133 | 332 | 130 | 324 | 80 | 317 | 158 | 313 | 158 | 314 | 80 | 317 | 161 | 314 | 162 | 314 | 157 | 313 | 156 | 313 | 162 | 313 | 160 | 314 |
| 72 Dublin | 134 | 326 | 118 | 318 | 144 | 312 | 145 | 311 | 141 | 311 | 144 | 312 | 144 | 312 | 146 | 312 | 157 | 310 | 154 | 310 | 160 | 311 | 157 | 311 |
| 4 Aberystwyth | 151 | 230 | 159 | 215 | 146 | 220 | 146 | 220 | 146 | 219 | 146 | 220 | 146 | 219 | 147 | 220 | 153 | 225 | 154 | 224 | 153 | 226 | 152 | 225 |
| 138 OD | 138 | 309 | 128 | 299 | 147 | 296 | 150 | 296 | 148 | 294 | 147 | 296 | 148 | 296 | 150 | 298 | 160 | 296 | 157 | 295 | 159 | 295 | 156 | 295 |
| 139 ON | 112 | 184 | 130 | 172 | 107 | 172 | 105 | 174 | 109 | 174 | 107 | 172 | 101 | 173 | 106 | 174 | 102 | 179 | 102 | 179 | 95 | 181 | 97 | 180 |
| 43 B | 144 | 154 | 162 | 150 | 134 | 147 | 136 | 147 | 133 | 147 | 134 | 147 | 136 | 148 | 136 | 147 | 128 | 149 | 130 | 150 | 127 | 148 | 128 | 148 |
| 48 F | 156 | 136 | 167 | 133 | 157 | 133 | 157 | 132 | 157 | 132 | 157 | 133 | 157 | 132 | 157 | 132 | 155 | 132 | 155 | 133 | 155 | 132 | 156 | 133 |
| 51 G | 136 | 123 | 146 | 121 | 143 | 120 | 143 | 120 | 145 | 121 | 143 | 120 | 143 | 120 | 143 | 120 | 143 | 120 | 142 | 120 | 144 | 121 | 144 | 121 |
| 133 Newlyn | 172 | 133 | 169 | 128 | 166 | 131 | 166 | 129 | 165 | 129 | 164 | 129 | 165 | 129 | 165 | 129 | 165 | 130 | 165 | 130 | 165 | 130 | 165 | 130 |
| Bristol Channel Region | | | | | | | | | | | | | | | | | | | | | | | | |
| 11 Aust | 415 | 210 | 435 | 223 | 374 | 231 | 426 | 215 | 406 | 222 | 362 | 233 | 365 | 232 | 435 | 211 | 426 | 201 | 430 | 200 | 427 | 201 | 430 | 204 |
| 12 Avonmouth | 430 | 200 | 430 | 221 | 268 | 228 | 419 | 213 | 402 | 221 | 356 | 228 | 359 | 228 | 430 | 210 | 424 | 200 | 427 | 200 | 424 | 201 | 427 | 203 |
| 25 Beachley | 417 | 211 | 435 | 223 | 374 | 231 | 426 | 215 | 406 | 222 | 362 | 233 | 365 | 232 | 433 | 211 | 426 | 201 | 430 | 200 | 427 | 201 | 430 | 204 |
| 56 Clevedon | 415 | 196 | 418 | 208 | 357 | 222 | 413 | 209 | 394 | 218 | 356 | 222 | 349 | 218 | 419 | 206 | 420 | 199 | 414 | 196 | 409 | 196 | 411 | 198 |
| 98 Inward Rocks | 394 | 223 | 435 | 223 | 374 | 231 | 426 | 215 | 406 | 222 | 362 | 232 | 365 | 232 | 433 | 211 | 426 | 201 | 430 | 200 | 427 | 201 | 430 | 204 |
| 153 Bristol | 426 | 202 | 430 | 221 | 268 | 228 | 419 | 213 | 403 | 221 | 357 | 229 | 359 | 228 | 426 | 209 | 424 | 200 | 427 | 200 | 424 | 201 | 427 | 203 |
| 210 Weston-s-M. | 443 | 195 | 407 | 200 | 369 | 196 | 386 | 197 | 372 | 198 | 372 | 196 | 373 | 198 | 396 | 192 | 391 | 189 | 397 | 191 | 390 | 189 | 392 | 191 |
| North Channel Region | | | | | | | | | | | | | | | | | | | | | | | | |
| 7 Ardminish Bay | 19 | 81 | 19 | 148 | 34 | 287 | 36 | 297 | 33 | 292 | 32 | 299 | 33 | 295 | 36 | 302 | 16 | 268 | 17 | 269 | 17 | 287 | 17 | 284 |
| 64 Craighouse | 23 | 85 | 21 | 165 | 35 | 287 | 38 | 298 | 32 | 288 | 28 | 287 | 31 | 291 | 31 | 291 | 21 | 247 | 18 | 233 | 20 | 266 | 20 | 264 |
| 100 Islay | 16 | 89 | 14 | 171 | 25 | 269 | 20 | 280 | 23 | 272 | 21 | 276 | 23 | 274 | 28 | 276 | 22 | 224 | 24 | 235 | 24 | 269 | 24 | 268 |
| 114 Loch Inver | 146 | 202 | 120 | 334 | 172 | 326 | 160 | 322 | 160 | 323 | 164 | 324 | 164 | 325 | 167 | 327 | 143 | 320 | 143 | 320 | 147 | 321 | 147 | 321 |
| 119 Macrahanish | 20 | 31 | 7 | 22 | 43 | 294 | 45 | 300 | 41 | 296 | 40 | 305 | 42 | 299 | 41 | 300 | 39 | 305 | 39 | 303 | 43 | 309 | 42 | 308 |
| 195 Stn D | 26 | 87 | 37 | 156 | 28 | 285 | 37 | 307 | 32 | 295 | 22 | 274 | 21 | 263 | 28 | 296 | 12 | 212 | 11 | 218 | 7 | 254 | 8 | 262 |
| 196 Stn E | 7 | 125 | 17 | 186 | 33 | 257 | 30 | 274 | 32 | 257 | 30 | 264 | 31 | 260 | 32 | 251 | 33 | 241 | 33 | 236 | 28 | 245 | 29 | 242 |

**Table 5** Water depths (m) at comparison points

| | Calc | | | | | | | | | |
|---|---|---|---|---|---|---|---|---|---|---|
| | BM | 1 | 2 | 3 | 4 | 5 | 6 | 7 | 8 | 9 | 10 |
| 20 Barrow | 9.0 | 10.1 | 5.2 | 4.3 | 9.9 | 6.1 | 9.8 | 10.2 | 9.8 | 9.1 | 9.1 |
| 89 Heysham | 10.0 | 8.9 | 7.7 | 3.3 | 10.8 | 7.8 | 5.1 | 9.9 | 10.0 | 5.6 | 5.6 |
| 90 Hilbre | 11.0 | 8.7 | 8.5 | 5.8 | 3.8 | 11.4 | 6.4 | 10.2 | 11.4 | 16.2 | 16.2 |
| 108 Liverpool | 15.0 | 9.9 | 12.9 | 9.0 | 9.0 | 6.6 | 0.0 | 15.2 | 14.6 | 14.6 | 15.1 |
| 110 Liverpool Bay | 13.0 | 12.5 | 12.9 | 12.6 | 10.3 | 10.6 | 10.0 | 12.5 | 12.4 | 11.2 | 11.2 |
| 128 Morecambe | 8.0 | 3.7 | 4.3 | 5.2 | 2.8 | 2.8 | 1.7 | 8.0 | 8.2 | 3.0 | 3.0 |
| 213 Workington | 11.0 | 7.3 | 10.2 | 7.1 | 10.5 | 10.4 | 9.2 | 11.8 | 16.1 | 10.8 | 10.8 |
| 163 Portpatrick | 45.0 | 53.6 | 60.6 | 24.8 | 0.0 | 15.5 | 27.2 | 53.6 | 46.8 | 77.4 | 77.4 |
| 11 Aust | 8.0 | 5.7 | 9.9 | 10.0 | 4.7 | 4.7 | 8.0 | 9.8 | 10.0 | 8.6 | 8.6 |
| 12 Avonmouth | 10.0 | 8.9 | 10.0 | 10.0 | 7.2 | 8.6 | 9.0 | 9.1 | 10.4 | 9.7 | 9.7 |
| 56 Clevedon | 11.0 | 9.9 | 10.5 | 10.0 | 4.7 | 5.6 | 10.3 | 12.1 | 10.5 | 10.7 | 10.7 |
| 210 Weston-s-M. | 16.0 | 13.0 | 11.2 | 10.0 | 8.3 | 7.6 | 16.0 | 11.2 | 14.0 | 11.9 | 11.9 |
| 100 Islay | 33.0 | 35.8 | 26.7 | 22.3 | 10.7 | 25.0 | 38.2 | 34.5 | 49.3 | 43.6 | 43.6 |
| 119 Macrahanish | 13.0 | 12.6 | 10.6 | 12.6 | 10.7 | 11.0 | 12.1 | 14.3 | 17.2 | 15.0 | 15.0 |

**Table 6** Number of points where computed elevation amplitude $h$ (cm) or phase $g$ (°) exceeds (+) or is below (−) the observed value. Also given are values of global error estimates

| Calc | | $<-30$ | $-30$ | $-25$ | $-20$ | $-15$ | $-10$ | $-5$ | 5 | 10 | 15 | 20 | 25 | 30 | $>30$ | Average deviation | RMS | $H_S$ | $\bar{H}_S$ | $H_{EX}$ | $\bar{H}_{EX}$ | Average deviation (EX) | RMS (EX) |
|---|---|---|---|---|---|---|---|---|---|---|---|---|---|---|---|---|---|---|---|---|---|---|---|
| BM | $h$ | 3 | 7 | 5 | 7 | 11 | 16 | 18 | 28 | 21 | 37 | 34 | 13 | 5 | 9 | 6.02 | 16.9 | 7,184 | 33.5 | 6,102 | 30.8 | 6.39 | 16.8 |
| | $g$ | 5 | 4 | 3 | 5 | 28 | 50 | 74 | 9 | 8 | 11 | 5 | 2 | 0 | 10 | −1.45 | 20.0 | | | | | −5.20 | 12.1 |
| 1 | $h$ | 6 | 6 | 7 | 12 | 8 | 18 | 16 | 30 | 24 | 21 | 14 | 6 | 10 | 36 | 7.40 | 24.3 | 10,201 | 47.6 | 8,552 | 43.1 | 9.14 | 20.9 |
| | $g$ | 4 | 6 | 14 | 20 | 45 | 35 | 41 | 6 | 14 | 6 | 6 | 1 | 3 | 13 | 1.66 | 41.6 | | | | | −7.23 | 15.7 |
| 2 | $h$ | 1 | 3 | 4 | 11 | 11 | 21 | 23 | 29 | 13 | 24 | 19 | 12 | 7 | 36 | 9.23 | 21.5 | 9,391 | 43.8 | 8,285 | 41.8 | 9.51 | 21.6 |
| | $g$ | 3 | 4 | 16 | 19 | 41 | 36 | 44 | 10 | 13 | 11 | 2 | 0 | 1 | 14 | 2.17 | 43.5 | | | | | −6.72 | 15.5 |
| 3 | $h$ | 7 | 4 | 12 | 6 | 15 | 19 | 15 | 26 | 29 | 18 | 12 | 9 | 6 | 36 | 6.21 | 24.3 | 10,007 | 46.7 | 8,680 | 43.8 | 6.95 | 24.4 |
| | $g$ | 3 | 5 | 14 | 18 | 45 | 36 | 41 | 9 | 7 | 11 | 9 | 3 | 0 | 13 | 2.24 | 42.1 | | | | | −6.50 | 15.8 |
| 4 | $h$ | 20 | 4 | 11 | 8 | 7 | 16 | 19 | 29 | 23 | 16 | 12 | 12 | 7 | 30 | −0.01 | 37.9 | 10,683 | 49.9 | 9,031 | 45.6 | 1.53 | 37.7 |
| | $g$ | 5 | 3 | 14 | 13 | 48 | 38 | 42 | 8 | 10 | 7 | 3 | 7 | 3 | 13 | 1.54 | 47.5 | | | | | −7.59 | 27.1 |
| 5 | $h$ | 17 | 7 | 11 | 10 | 12 | 14 | 13 | 28 | 27 | 13 | 16 | 10 | 5 | 31 | −1.20 | 42.9 | 10,847 | 50.6 | 9,228 | 46.6 | 0.24 | 43.1 |
| | $g$ | 5 | 4 | 13 | 13 | 46 | 39 | 41 | 7 | 11 | 10 | 1 | 6 | 5 | 13 | 1.55 | 47.0 | | | | | −7.42 | 27.1 |
| 6 | $h$ | 14 | 2 | 3 | 4 | 10 | 18 | 20 | 30 | 20 | 25 | 15 | 13 | 8 | 32 | 3.39 | 37.9 | 9,747 | 45.5 | 8,713 | 44.0 | 2.87 | 39.0 |
| | $g$ | 5 | 4 | 11 | 11 | 42 | 47 | 41 | 20 | 7 | 7 | 2 | 1 | 2 | 14 | 1.37 | 49.2 | | | | | −7.23 | 29.9 |
| 7 | $h$ | 3 | 5 | 5 | 3 | 16 | 16 | 24 | 21 | 18 | 21 | 17 | 19 | 23 | 23 | 8.66 | 20.0 | 8,476 | 39.6 | 7,519 | 37.9 | 9.16 | 20.2 |
| | $g$ | 4 | 4 | 17 | 21 | 38 | 34 | 47 | 26 | 4 | 3 | 1 | 0 | 1 | 14 | −0.39 | 36.1 | | | | | −7.17 | 15.1 |
| 8 | $h$ | 6 | 2 | 3 | 6 | 13 | 15 | 22 | 20 | 24 | 19 | 24 | 21 | 17 | 22 | 9.01 | 19.7 | 8,419 | 39.3 | 7,478 | 37.7 | 9.44 | 19.8 |
| | $g$ | 4 | 4 | 15 | 23 | 41 | 29 | 49 | 24 | 6 | 2 | 1 | 1 | 1 | 14 | −0.02 | 36.4 | | | | | −6.85 | 15.1 |
| 9 | $h$ | 6 | 6 | 4 | 10 | 10 | 17 | 22 | 22 | 12 | 17 | 23 | 18 | 18 | 29 | 7.78 | 26.8 | 8,157 | 38.1 | 7,209 | 36.4 | 8.23 | 27.3 |
| | $g$ | 2 | 5 | 16 | 14 | 32 | 38 | 55 | 25 | 7 | 3 | 1 | 0 | 1 | 15 | 1.93 | 40.1 | | | | | −5.78 | 14.2 |
| 10 | $h$ | 4 | 6 | 4 | 8 | 11 | 17 | 22 | 25 | 17 | 18 | 22 | 18 | 18 | 24 | 7.51 | 26.0 | 8,031 | 37.5 | 7,112 | 35.9 | 7.86 | 26.4 |
| | $g$ | 2 | 5 | 15 | 13 | 35 | 36 | 52 | 27 | 8 | 4 | 1 | 0 | 1 | 15 | 2.14 | 40.0 | | | | | −5.60 | 14.2 |

comparable resolution namely of the order of 7 km between nodes, to the finite difference grid, enabling the two to be compared. In both calculations the nearest computed point to the observation was used in the comparison. No attempt was made to interpolate to the observed point. Obviously in the case of an offshore observational point surrounded by finite element nodal points or in the finite difference grid where grid point values exist interpolation is possible. This would be based on the functional form of the finite element, or linear interpolation in the finite difference grid which is consistent with how gradients were approximated with this model. However, to be consistent with previous finite difference work and comparisons in coastal regions (see below) only nearest computed points were used. For coastal gauges often located within estuaries or very nearshore the observational point is at the edge or outside the finite element or finite difference domain, and unless a very fine nearshore grid is used it is not surrounded by computational values and interpolation is not possible. A comparison with the nearest point, and how the location of this point changes, with associated changes in water depth and computed tide, as the finite element grid is refined, is then a useful indication of the effect of grid resolution upon the accuracy of tides in the nearshore region. Consequently some differences between models arose due to comparison points being at different locations. However, this is reasonable in that it reflects the finite resolution of the model. In this initial finite element calculation the bottom topography and

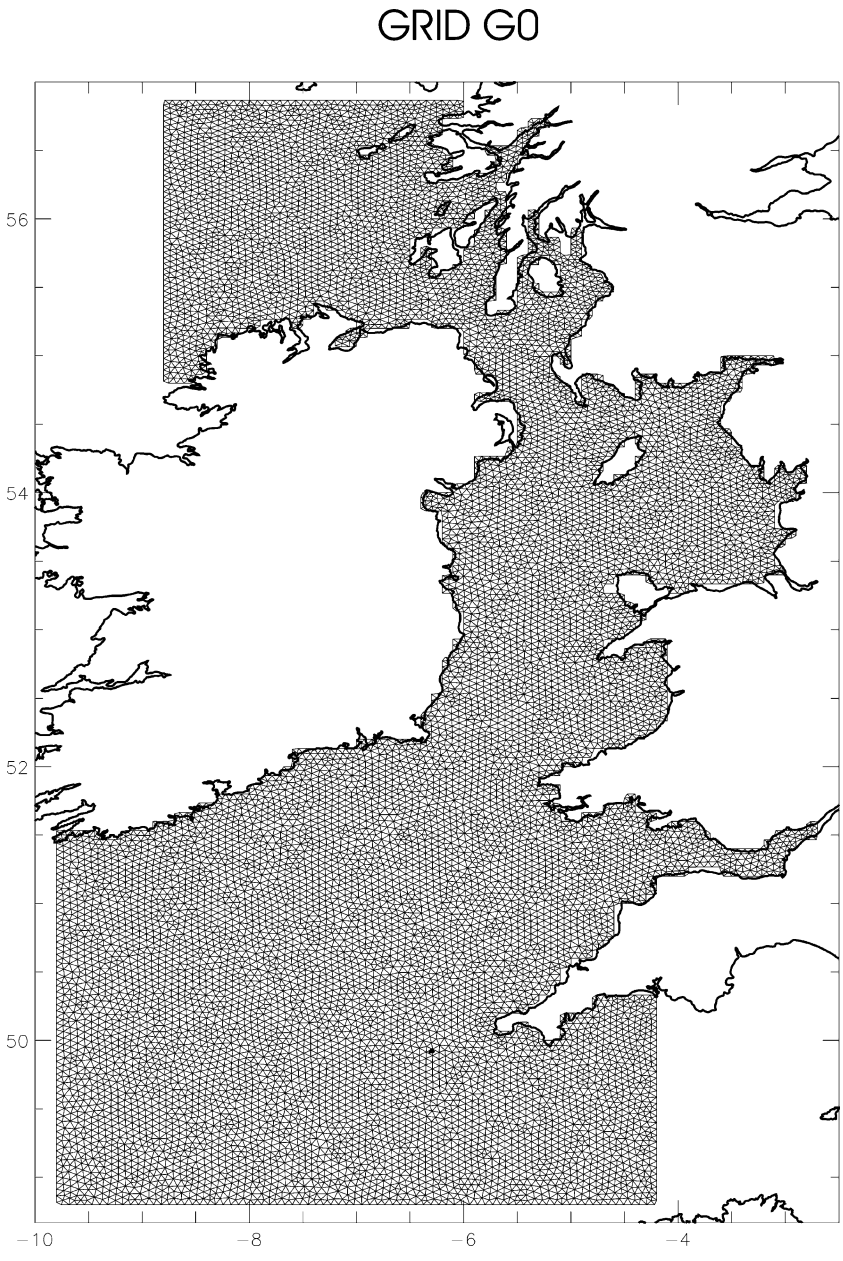


**Fig. 4** The uniform finite element grid (GO), used in Calc 1

open boundary forcing were as previously. In addition the same coastal representation was used to obtain a 'like with like' comparison. A consequence of this was that rather than following the true coastline as accurately as possible, the finite difference coastal description was used. In addition in the initial set of calculations the water depth at the coast was set to zero. Consequently in the near coastal elements the water depth varied linearly from non-zero offshore to zero at the coast. In the comparison with coastal gauges where the nearest nodal point in the finite element mesh was used, this meant that the water depth at this location was different from that in the finite difference model (Table 5). Also in shallow regions significant 'wetting and drying' occurred with an associated loss of energy to higher harmonics (Fortunato et al. 1977, 1999) and increase in computational time (Table 2) associated with a rise in the number of iterations required to obtain a converged solution. Also since the average near coastal depth is shallower than in a calculation where the water depth is non-zero at the coast this changes the nearshore dynamics in particular the bottom friction effect. These problems will be discussed later in connection with the various calculations.

The computed cotidal chart (not shown) was not significantly different except in the North Channel from that determined with the finite difference model. In the finite element model the amphidromic point in the North Channel shown in Fig. 3 did not appear. The cotidal chart suggested a degenerate amphidrome situated on the Scottish coast, namely too far to the northwest. Idealized calculations (Davies and Jones 1995) have shown that the location of amphidromes is sensitive to changes in water depth distribution and

bottom frictional effects. In this narrow channel which is close to land, differences in the representation of nearshore water depths between the finite element and finite difference model will clearly have a local effect. Also, a recent calculation with a high resolution (of order 1 km) limited area model of the region (Davies et al. 2004) has shown that the amphidromic point in this region is very sensitive to small changes in the tide off the west coast of Scotland and in the Irish Sea. This suggests that the exact location of the North Channel amphidrome is influenced by local resolution and small changes in tidal distribution to the north and south of the region. The inaccuracy in the computed tide in the North Channel is reflected in the overprediction of tidal amplitudes and phases in this region (Calc 1, Table 4).

At offshore tide gauges in the Celtic Sea, particularly B, F, G the calculation gives lower amplitudes than those found in the finite difference model (Calc BM, Table 4). However, within the Irish Sea, and in particular in the eastern Irish Sea at offshore gauges Q, S, U, V, the amplitude is larger, and phase smaller than that computed with the finite difference model. This increase in offshore amplitude is reflected in the increased amplitude at coastal gauges in the eastern Irish Sea, which are on average 10 cm higher. A consequence of this is that the finite difference solution is in slightly better agreement with observations than the finite element model. Also the phase is reduced in the finite element model leading on average to a reduction in accuracy compared to the finite difference model. This increase in amplitude and change in phase compared to the finite difference model may be due to the fact that the finite element model as used here represents coastal topography by a linear reduction in water depth, rather than a flat constant depth region and vertical wall. This would increase amplitude and reduce phase in the near coastal region.

In the Bristol Channel, tidal amplitude is reduced compared to the finite difference calculation (Calc BM, Table 4). This is due to the fact that in many regions there are perhaps only two elements across the channel. As discussed previously the water depth in the finite element reduces to zero at the coast. Consequently the average across channel water depth is substantially less than in the finite difference model. This reduces the flow into the estuary, leading to a decrease in amplitude. The smaller water depth enhances bottom friction leading to a reduction in amplitude and change in phase. In addition with a zero water depth at the coast there is significant 'wetting and drying'. This together with the rapid spatial variations in currents in the region leads to appreciable generation of higher harmonics with a corresponding loss of energy from the $M_2$ tide. An accurate description of the bottom topography with sufficient precision to allow for the correct representation of the tidal flats as shown by a number of authors (Fortunato et al. 1997, 1999; Heniche et al. 2000) is essential to account for the energy loss from $M_2$ to the higher harmonics. In the present model the resolution is too coarse in the Bristol Channel.

To examine to what extent a local refinement in the North Channel and Bristol Channel had on the tide in these regions and elsewhere a locally refined grid (Grid G1) was generated (Table 1). This grid was identical to GO, except in the North Channel and Bristol Channel areas, where a uniform grid of 1 km resolution was used (Grid G1).

Computed amplitudes and phases in the North Channel (Calc 2, Table 4) show an increase in amplitude at Craighouse, Loch Inver and Stn D, compared with Calc 1. Similarly in the northern Irish Sea, namely Belfast and Port Patrick, tidal amplitudes increase, although farther south (Aberystwyth) and in the Celtic Sea there is little change. This suggests that additional tidal energy is entering the Irish Sea due to the improved resolution in the North Channel. The importance of the North Channel in determining the energy flux into the Irish Sea was recently shown by Davies et al. (2004). The fact that this energy flux does not have a large influence in the Celtic Sea, is due to the fact that in the Irish Sea, the main energy flux is into the shallow water region of the eastern Irish Sea (Davies and Kwong 2000) where maximum dissipation occurs. The increased energy flux into the eastern Irish Sea, resulting from the improved resolution in the North Channel, is reflected in the slight increase in amplitude at coastal gauges in the region (compare Calcs 1 and 2 in Table 4). At coastal ports such as Heysham and Liverpool tidal amplitude increases on average by 3 cm. However, at other ports, for example, Morecambe the tidal amplitude decreases and phase increases by 8°. These changes are in part due to the fact that refining the grid in the North Channel, leads to a slight modification of the grid elsewhere. Consequently, the nearest nodal point in the mesh to the comparison point changes its location slightly, as is evident from the water depths at comparison points given in Table 5. This will be discussed in more detail later.

The local increase in amplitude and decrease in phase within the Bristol Channel (compare Calcs 1 and 2 in Table 2) is primarily due to an increase in the across channel water depth in the region, when the grid is refined in the Channel. This allows an increased tidal energy flux into the region, and an improved description of the tidal propagation in the estuary. In addition an increase in water depth affects the extent of the 'wetting and drying' region and hence the energy loss from the $M_2$ tide is reduced. The enhanced energy flux and change in 'wetting and drying' is reflected in the increase in amplitude and change in phase in the Bristol Channel region between Calcs 1 and 2 (Table 4). It is important to note that in this area because the grid has changed, and as discussed previously to be consistent with the finite difference calculation we are using nodal values, identical positions are not being compared. However, the fine nature of the original grid in the region means that locations have not moved over large distances. This will be discussed later in connection with other calculations.

In these calculations the background grid was uniform and comparable to the finite difference grid. In a subsequent calculation (Calc 3, Table 4), an irregular grid (Grid G2) with about the same number of nodes as GO was generated. However, in this grid the ratio of grid size to $(gh)^{1/2}$ was nearly constant. This gave a grid resolution based upon the speed of propagation of free surface gravity waves. Consequently, the grid was finer in the near coastal regions although coarser offshore (Fig. 5).

The computed cotidal chart derived with this grid (Calc 3, Table 1) was not substantially different to that found with the uniform grid (GO). In the North Channel there is evidence of a degenerate amphidrome situated on the island off the Scottish coast to the north of Ireland. Comparison with high resolution models of the region (Davies et al 2001a, 2004) and cotidal charts based on observations (George 1980) suggests that this amphidrome is located too far to the northwest.

Comparing tidal amplitudes and phases in this region with those found in Calcs 1 and 2 (Table 4), suggests a solution which on average is of comparable accuracy. The improved (compared to Calc 1) resolution in the region appears to allow more energy to enter the Irish Sea. This is evident at the Irish Sea ports of Belfast, Port Patrick, Dublin and Aberystwyth, where amplitude and phase are in close agreement with those found in Calc 2 (refined grid resolution in the North Channel).

In the near coastal regions of the eastern Irish Sea the finite element grid (G2) used in the calculation is significantly finer (of the order of 100 m compared with 7 km) than in the uniform grid (compare Figs. 4, 5). This has the effect of improving resolution in the shallow water region where tidal energy is dissipated. A conse-

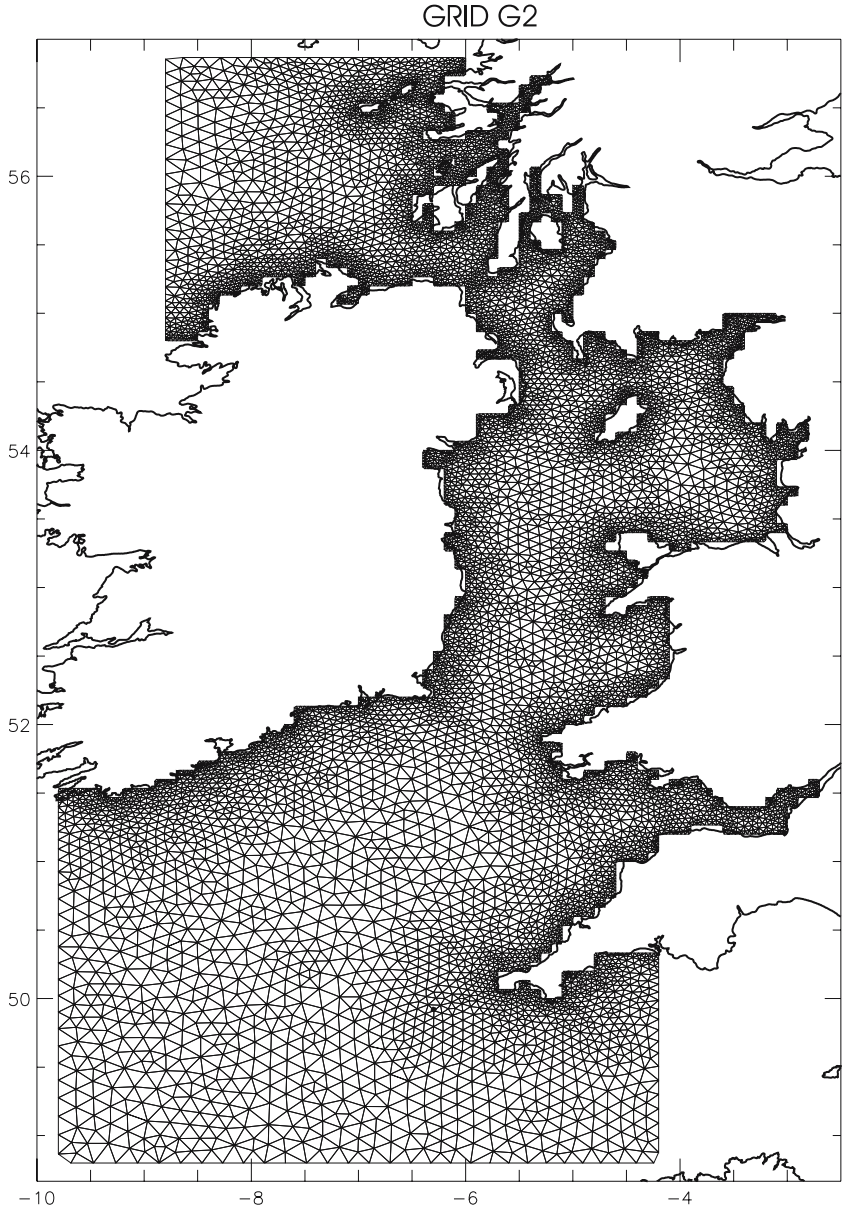


**Fig. 5** The irregular finite element grid (G2) used in Calc 3

quence of this is that tidal amplitudes are reduced in the eastern Irish Sea compared with Calc 2 (compare Calcs 2 and 3 in Table 4). This suggests that tides in the eastern Irish Sea are sensitive to both the energy flux into the region, which can be influenced by North Channel resolution and by resolution in the near coastal region.

Tidal amplitudes in the Bristol Channel as shown in the comparison between Calcs 1 and 2 are sensitive to local resolution. This is confirmed by the results from Calc 3, which at some locations (not shown) are below those found in Calc 1, and at others between Calcs 1 and 2. This reflects the local changes produced by local refinements of the grid in this region. However, on average results using grid G2 (Calc 3) are only slightly improved on those using GO (Calc 1), as illustrated by the RMS, $\bar{H}_S$ and histograms shown in Table 6. This suggests that in order to improve the model's accuracy, more detailed nearshore topography is required. Without improved topography in the near coastal region and a better coastal representation then the benefits of a graded mesh are small.

In this series of calculations the bottom topography and coastal description were taken from the west coast model finite difference grid. This was done so that direct comparisons with that model were possible. Calculations showed that the tidal distribution in the eastern Irish Sea was critically dependent upon resolution in that area. In the next section the eastern Irish Sea grid and coastline are refined using topography from the high-resolution eastern Irish Sea model of Jones and Davies (1996).

## Finite element models with enhanced topography in the eastern Irish Sea

In this calculation (Calc 4, Table 1) the topography in the eastern Irish Sea was taken from the 1 km model of Jones and Davies (1996). The finite element grid (Grid G3, Table 1) (Fig. 6) was determined from this topography with an identical criterion to that used for grid G2. However, the improved nearshore topography in the eastern Irish Sea, led to a significantly better (in that bathymetry on a 1 km rather than 7 km grid was available) representation of the coastline in this region (compare Figs. 5, 6).

The computed co-amplitude and co-phase charts have the same large-scale characteristics as those determined with grid G2, although there has been a change in the eastern Irish Sea (Fig. 7), due to the improved topography in this region. Including a better representation of the near coastal shallow water regions in some locations leads to an increase compared with Calc 3 in tidal amplitude and phase (compare eastern Irish Sea ports Barrow, Hilbre in Table 4). However, at other locations in the eastern Irish Sea, for example, Liverpool, Morecambe, amplitude and phase have decreased (Table 4 compare Calcs 3 and 4). At offshore gauges there has been very little change in amplitude or phase, suggesting that grid refinement only has a local effect.

Since, for reasons stated earlier, comparisons at gauges are made with the nearest offshore node in the finite element model, then refining the grid in the nearshore region will affect the water depth most in the coastal region. In addition as a zero water depth is specified at the coast and in this series of calculations this is used to interpolate water depths, then coastal values of depth will change significantly between Calcs 3 and 4. This is illustrated in Table 5. It is evident at eastern Irish Sea ports such as Barrow, Heysham and Workington that the water depth at the finite element node used in the comparison has increased. However, at other locations namely Hilbre, Liverpool, Liverpool Bay and Morecambe it has decreased. These changes in water depth at comparison points, together with the improved description of the coastal topography explain the differences in amplitude and phase between Calcs 3 and 4.

Although the water depth is only changed in the eastern Irish Sea, the criterion used to generate the mesh means that the location of nodes and hence comparison points changes over the whole region. A consequence of this, and the comparison criterion used, namely that the nearest node to the observation point is used in the comparison means that in certain regions, for example, the North Channel or Bristol Channel water depths at comparison points change very significantly (Table 5). For example, in the North Channel region the water depth at the Port Patrick comparison point changes from 24 m to less than 1.0 m as the nodal point moves slightly closer to the coast due to the 'knock on' effect of the grid refinement in the eastern Irish Sea. This has an appreciable influence upon computed tidal amplitude at this node which is reduced from 158 cm to 80 cm. However at other locations where the water is deeper, for example, Islay where the water depth changes from 22.3 to 10.7 m, tidal amplitude only decreases slightly, namely 23–21 cm.

The most significant change in tidal amplitude due to a very small (of order 10 m) adjustment of the local grid produced as a 'knock on effect' of the eastern Irish Sea re-gridding occurs in the Bristol Channel (see Table 4). Besides a small change in grid location, water depths in the area are reduced. In this region tidal amplitudes are reduced by the order of 40 cm, and phases increase by about 10° (compare Calcs 3 and 4 in Table 4). This change is due to an appreciable reduction in water depths at the comparison points in the region (Table 5). In the deeper water regions of the Bristol Channel although there are small changes in the location of nodal points and average water depth, this has little effect upon the tide.

This comparison clearly shows, as is to be expected, that changing the topography in the eastern Irish Sea changes the tide in this area, but not in the western Irish Sea and Celtic Sea regions. However the fact that the associated re-gridding modifies the grid in regions such as the Bristol Channel means that comparisons with observational points in this area are changed. The sen-

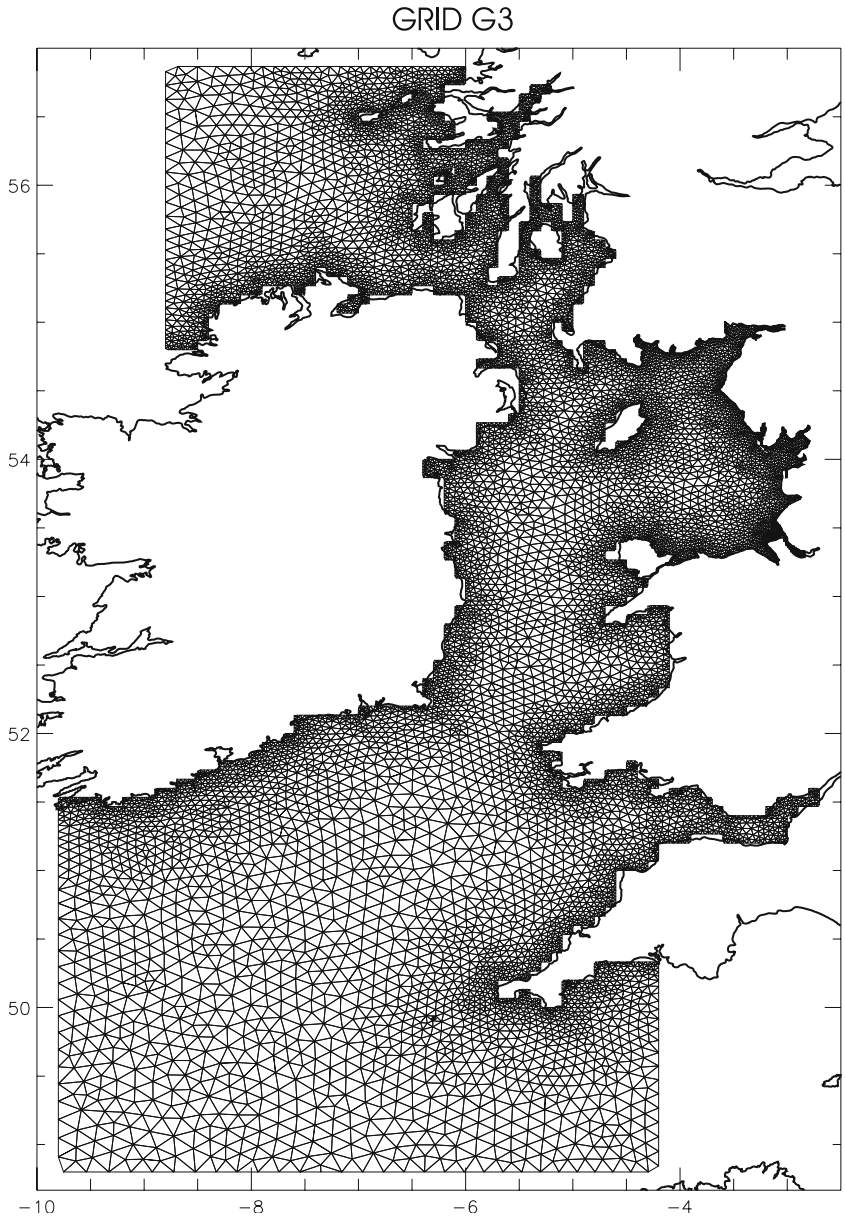


**Fig. 6** The irregular finite element grid (G3) used in Calc 4

sitivity of tides to changes in local bathymetry is considered in the next two calculations.

Although the topography and coastal representation has been improved in this calculation compared with the earlier one (Calcs 1–3) it is evident from Table 6 that there has been no improvement in overall accuracy. Even when the poorly resolved regions (i.e. North Channel and Bristol Channel) are removed from the comparison, there is no improvement in the solution. This suggests that the coastal boundary condition of zero water depth is probably not appropriate. A revised condition is considered in the next section.

In Calc 5 (Table 1) the topography was as previously but a finer mesh was used in the Mersey estuary. As discussed previously this causes the grid over the whole region of the model to be slightly modified with major changes occurring in the Eastern Irish Sea. In addition changes do occur outside the area with associated modifications of water depth at nodal points used in the comparisons (Table 5). Refining the grid in the Mersey Estuary leads to water depths below 1 m at Liverpool (Calc 5, Table 5) with a resulting spurious tidal amplitude at this point (Calc 5, Table 4). The change in mesh in the eastern Irish Sea due to the refinement in the Mersey, influences water depths at some nodal positions, for example, Barrow, Hilbre (compare Calcs 4 and 5 in Table 5) with an associated change in tide (Table 4). However at other points, for example, Morecambe, Workington water depth hardly changes (compare Calcs 4 and 5 in Table 5), but the tidal signal changes at Morecambe (tidal amplitude increases from 267 to 293 cm, Table 4) due to water depth changes in the region.

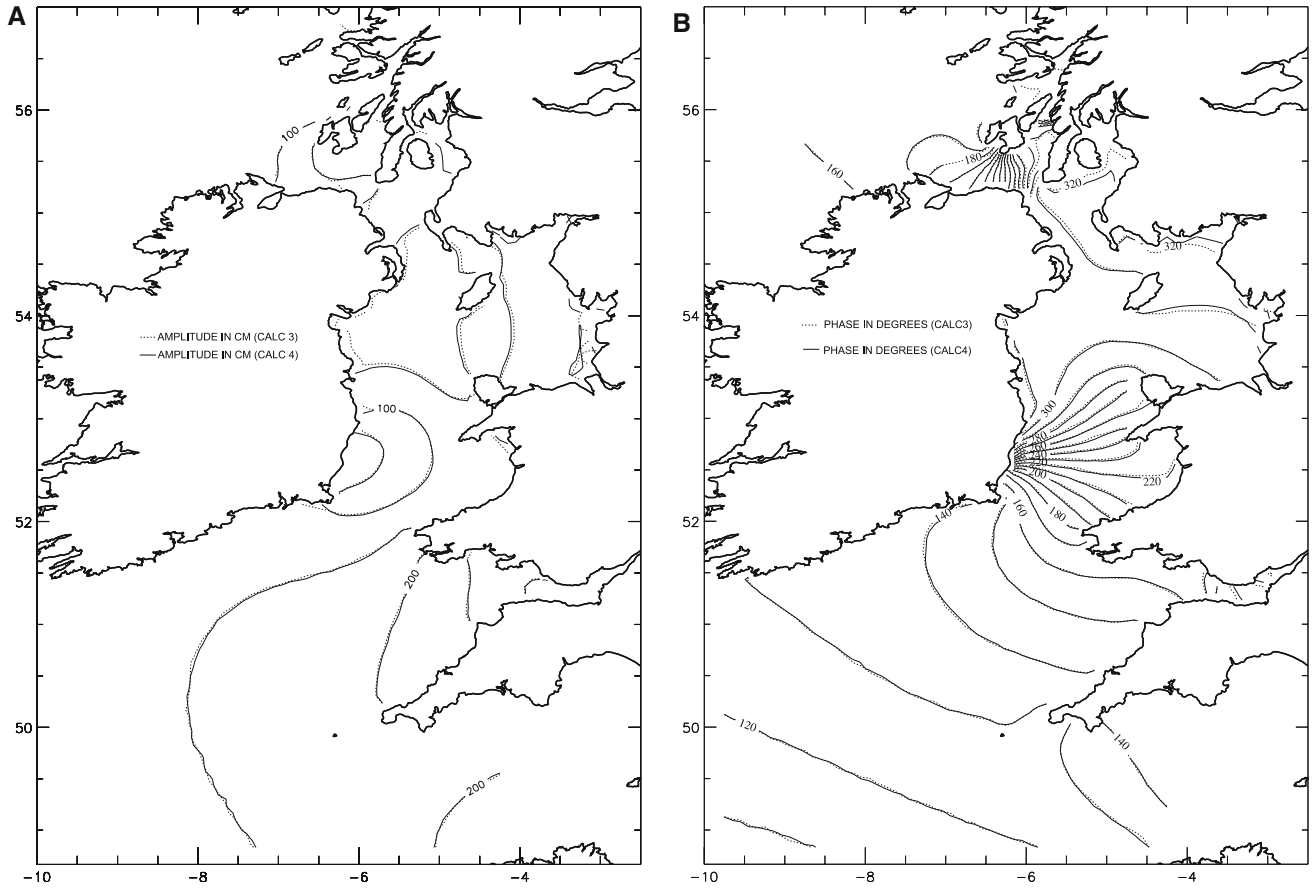


**Fig. 7** (a) Co-amplitude and (b) co-phase charts derived from Calcs 3 (dotted line) and Calc 4 (solid line)

In deeper areas namely offshore tide gauges in the eastern Irish Sea, and gauges in the Celtic Sea there is not a major change in the tide between Calcs 4 and 5 (see Table 4). Slight changes in the mesh due to refinement in the Mersey do however modify water depths at comparison nodes in the Bristol Channel with a resulting change in computed tide at these locations (Table 4). In terms of overall accuracy the $\bar{H}_S$ error increases slightly compared to previously, and there is still a significant bias in the model to overpredict amplitudes and underpredict phases (see histograms in Table 6).

To examine to what extent refining the mesh in the Bristol Channel had upon the local tide and that in the west coast region, in Calc 6 (Table 1) a finer resolution grid of the Bristol Channel was included. Outside this region the topography was identical to that used in grid G3. The effect of modifying the grid in the Bristol Channel was to change water depths at the nearest nodes to the observational point (Table 5). The average effect of refining the grid in the region was to increase the water depth between the order of 4–8 m (compare Calcs 6 and 4 in Table 5). The effect of this rise in water depth was to increase amplitudes and reduce phases (compare Calcs 6 and 4 in Table 4). This refinement of the mesh in the Bristol Channel reduces the value of $\bar{H}_S$ and the bias in the model to overpredict tidal amplitudes, although not phases (See Table 6).

The slight change in grid in the eastern Irish Sea due to the refinement in the Bristol Channel, leads to a modification in position of nodal points used in the comparison. Associated with this change in position is a depth change at near coastal points, for example, Liverpool node water depth 6.6 m in Calc 4, but 15.2 m in Calc 6. These changes in position of comparison points leads to a difference in tide at these locations compared to previously (compare computed tides from Calcs 6 and 4 in Table 4).

These calculations clearly show that global changes in the mesh due to local refinement, mean that the location of nearest nodes to observational points used to determine model accuracy change their position. Since the water depth in the nearshore region is determined by linearly interpolating between a given offshore water depth, and zero at the coast, changes in nodal position affect the nearshore distribution of water depth and hence tide. To try to reduce this sensitivity and examine its implication an alternative approach is adopted in the next section.

## Specification of coastal water depth and use of higher order element

In this series of calculations (namely Calcs 7 to 10, Table 1) instead of specifying a zero water depth at the

coast as in the previous calculations, a coastal depth was extrapolated from offshore depths. In Calc 7 a grid GOX (Table 1) with uniform elements that were identical to those in grid GO was generated. Although, in this grid water depths at the coast were non-zero, the no normal flow condition at land was still satisfied. Although the number of nodes and elements were identical to those in grid GO, the associated time was significantly reduced (Table 2), due to a reduction in the number of iterations required to obtain a converged solution. The number of iterations was related to the fact that with zero coastal water depth there was the potential for 'wetting and drying' in large areas of the coastal region which required additional computation.

Water depths at a number of nearshore comparison points (Table 5, Calc 7) were on average deeper than those in GO (Calc 1), due to the use of non-zero depths at the shore. This increase in nearshore depth gave a larger volume comparable to the finite difference model (Calc BM). In the eastern Irish Sea on average tidal elevation amplitude increased compared to grid GO (see Table 4, compare Calcs 1 and 7), although the change in phase was small (of order 1°).

In the Bristol Channel region which was poorly resolved with the GO grid, the use of a zero water depth at the coast gave water depths that were too low. In addition there was significant 'wetting and drying' with appreciable energy loss from the $M_2$ tide. This gave rise to the underprediction of tidal elevation amplitude that is evident in Table 4 (Calc 1). However, amplitude increases, and phase is reduced giving a significantly better agreement with observations when GOX is used (compare Calcs 1 and 7 in Table 4). It is apparent from Table 4, that amplitudes from Calc 7, are comparable to those from Calc 2 (Grid G1, a fine grid in the Bristol Channel) although phases are about 10° lower.

In the North Channel, amplitudes are significantly smaller than those computed with the GO grid (Calc 1), and in much better agreement with observations (see Table 4). Although phases are reduced on average by about 20° from those found in Calc 1 (Grid GO), they are still more than 180° different from the observed due to the inability of the model to predict the correct location of the amphidromic point in this region. The goodness of fit parameter $\bar{H}_S = 39.6$ (Calc 7, Table 6) is appreciably smaller than that found in previous calculations. Also the bias found previously in the elevation histograms to overpredict the elevation is significantly reduced. Within an accuracy criterion of $\pm 10$ cm, it is evident (Table 6, Calc 7) that there are 39 locations where elevation is overpredicted compared with 40 locations where it is underpredicted. However, the bias to underpredict the phase remains. This improvement in accuracy, together with the reduction in computer time suggests that the specification of a zero water depth at the coast with coarse elements in the coastal region is less accurate than extrapolating water depths to the coast. If however a water depth dependent criterion is used as in Calcs 3–6, with a non zero coastal water depth then the finite element mesh in the coastal region will be coarser. The consequences of this are examined in subsequent calculations.

In Calc 8 the topography was identical to that used in the west coast model and a grid G2X (Table 4) was generated by applying the same criterion as that used to produce grid G2. Since both grids are based on the west coast model geometry, they have an identical representation of the coastline. However, since in G2X the coastal water depth is non-zero, the finite elements in the nearshore region (Fig. 8) are not as small as in grid G2 (Fig. 5). However, in offshore regions the two grids are comparable. The reduction in number of near coastal elements is evident from the number of nodes and elements given in Table 2 (compare G2 and G2X) and the associated run times. The run time was significantly reduced not only because of the smaller number of elements, but also the number of iterations per time step required to reach a converged solution decreased. The effect upon water depth at comparison nodes can be readily seen in Table 5 (compare Calcs 8 and 3). By using a non-zero water depth at the coast, depths at comparison nodes in grid G2X are generally larger than those in G2. Also they are comparable to those at comparison points in the west coast finite difference model.

This difference is reflected in the differences in computed tide between Calcs 3 and 8 in Table 4, with elevation amplitudes tending to be larger in Calc 8. The exception to this is in the North Channel region. This appears to be due to a change in co-amplitude and co-phase lines in this region (compare Figs. 7, 9) due to differences in grid resolution between G2 (Fig. 5) and G2X (Fig. 8). The improvement in the overall accuracy of the computed tidal distribution is reflected in the decrease in the 'goodness of fit' parameters $\bar{H}_S$, $\bar{H}_{EX}$ and reduction in RMS error between Calcs 3 and 8 (Table 6). Although errors are still larger than those computed with the west coast model, it is evident that the bias in the histogram of elevation errors is reduced in Calc 8 compared with the finite difference model (Calc BM) and Calc 3. In particular in Calc 8, there is a fairly uniform distribution of elevation errors, with only a slight bias to overpredict the elevation. However, in both Calc 3 and Calc BM there is a significant bias to overpredict the elevation. In terms of phase, all the calculations have a bias to underpredict the phase, although this is largest in the BM calculation.

To examine the influence of improving the topography in the eastern Irish Sea, a grid G3X was generated using the same water depths as in G3, but with non-zero values at the coast. The improvement in coastal resolution in the eastern Irish Sea, due to using water depths based on a 1-km rather than 7 km resolution, is clearly evident from a comparison of Figs. 8 and 10. Although a water depth value is now specified at the coast, the fact that the eastern Irish Sea water depths have now been refined to include the shallow water regions means that there is not a significant difference in nearshore grid

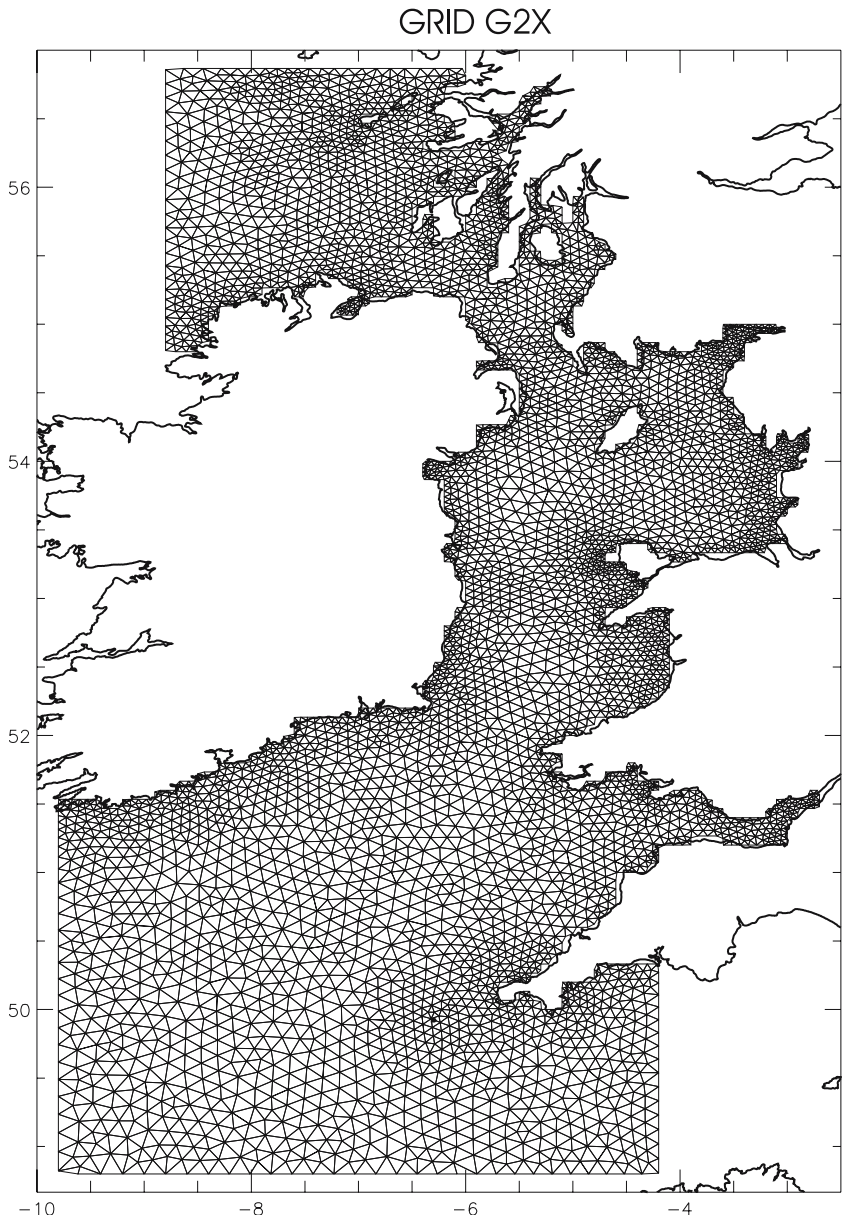


**Fig. 8** The irregular finite element grid (G2X) with non-zero coastal water depths used in Calc 8

resolution in the eastern Irish Sea between G3 and G3X (compare Figs. 6, 10). However, outside this region where the west coast finite difference model water depths are used the grid is comparable to G2X. The specification of a non-zero coastal water depth, reduces the number of elements (Table 2) from 21,018 (Grid G3) to 12,265 (Grid G3X). The reason that the number of elements in G3X is larger than Grid G2X (9,604), is due to the increased coastal resolution in the eastern Irish Sea.

On average computed tidal elevation amplitudes (Calc 9, Grid G3X) are increased (Table 6) above those determined with Grid G3 (Calc 4) although there is not a major change in phase (compare Calcs 9 and 4 in Table 4). This leads to an improvement in the 'goodness of fit' parameter $\bar{H}_S$ from 49.9 (Calc 4, Table 6) to 38.1 (Calc 9, Table 6) and a comparable reduction in $\bar{H}_{EX}$, resulting in an improvement in accuracy in the finite element solution. Although the $\bar{H}_S$ value is still larger than in the BM calculation, the bias in the elevation histogram is very small (Table 6). This can be clearly seen if the number of locations lying within $\pm 10$ cm is considered. Using this criterion, then in Calc 9 there are 34 locations overpredicted and 39 underpredicted, compared to 49 and 34 in the BM calculation (Table 6). Using the same criterion for phase gives 32 and 93 (Calc 9), with 17 and 124 (BM). Consequently, the same bias in phase is found in Calc 9 as in the BM Calc although the bias is reduced. As shown in other Irish Sea calculations (Davies et al. 2001b) two dimensional $M_2$ only calculations have a number of physical deficiencies. In particular the neglect of other tidal constituents reduces the frictional effect in the model. In addition relating bed stress to depth-mean current rather than bottom current as in a three dimensional multi-constituent calculation is

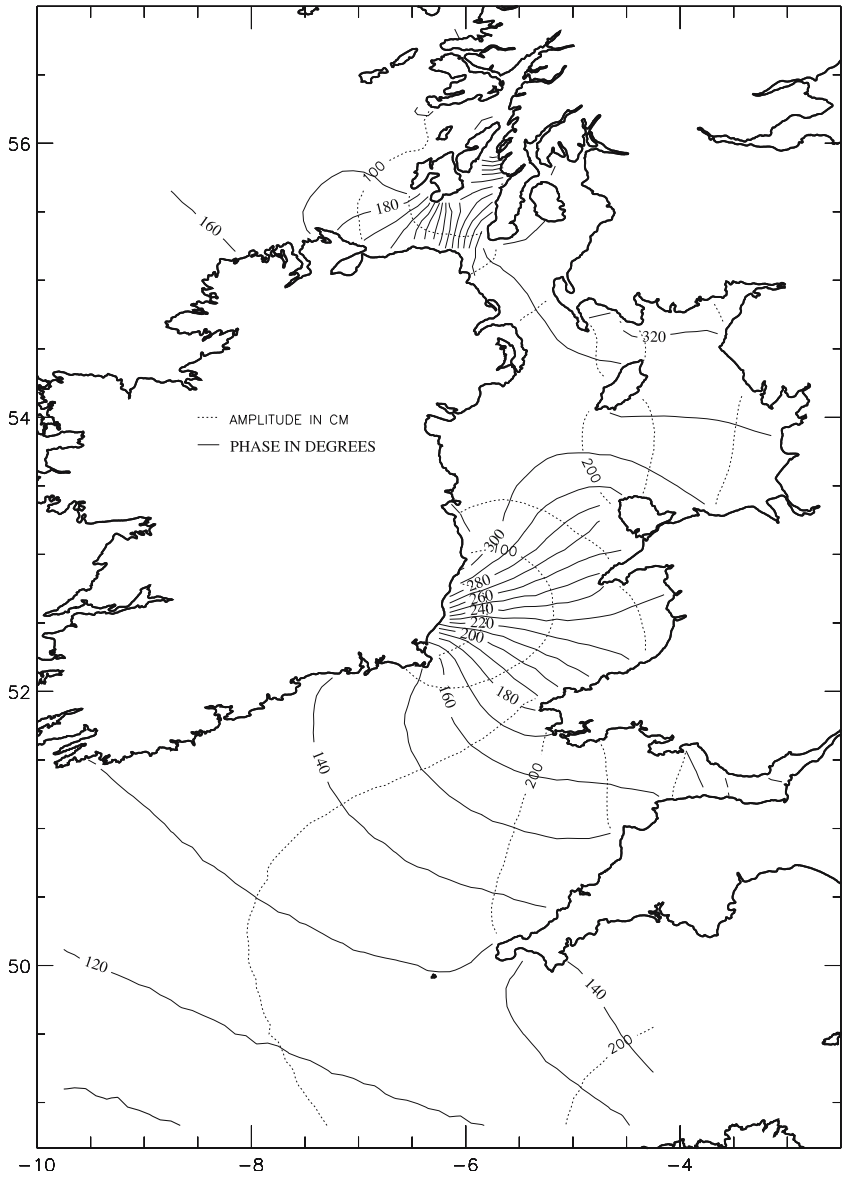


**Fig. 9** Computed $M_2$ co-tidal chart derived from Calc 8

a major deficiency in the model. These deficiencies in the formulation of a two-dimensional model go some way to explaining why there is a bias in phase, when an unbiased elevation distribution is obtained.

In a final calculation (Calc 10, Table 1) a higher order finite element, namely one with an additional pressure node at the centre of each triangle, was used with grid G3X. As only the order of the element was changed the water depths at comparison points were as before, as were the number of nodes and elements. The application of a higher order element did however slightly increase the computer time (Table 2).

However, the use of the higher order element led to a small (on average 3 cm in amplitude and 2° in phase) change in tidal elevation amplitude and phase in the Irish Sea although in the deeper waters of the Celtic Sea the change was not significant (Table 4). Similarly in the Bristol Channel, amplitude and phase increased by 3 cm and 3°, giving a slightly better agreement than previously. In the Bristol Channel region the amplitudes in Calc 10 were in slightly better agreement than those found with the west coast finite difference model (Calc BM), with a substantial improvement in phase (Table 4). Although the water depths in the region were based on those used in the west coast model, it is apparent that the improved resolution provided by the finite element mesh significantly enhanced the accuracy in the region.

In the North Channel area where the finite element grid is coarse and changes in water depth are very rapid, then using the higher order element at some locations changes the phase by the order of 20° (compare locations Craighouse and Islay Calcs 9 and 10 in Table 4). However at other locations the change is small.

The overall accuracy of the model is improved slightly (compare Calcs 9 and 10 in Table 6) with $\bar{H}_S$ being reduced from 38.1 to 37.5. A comparable reduc-

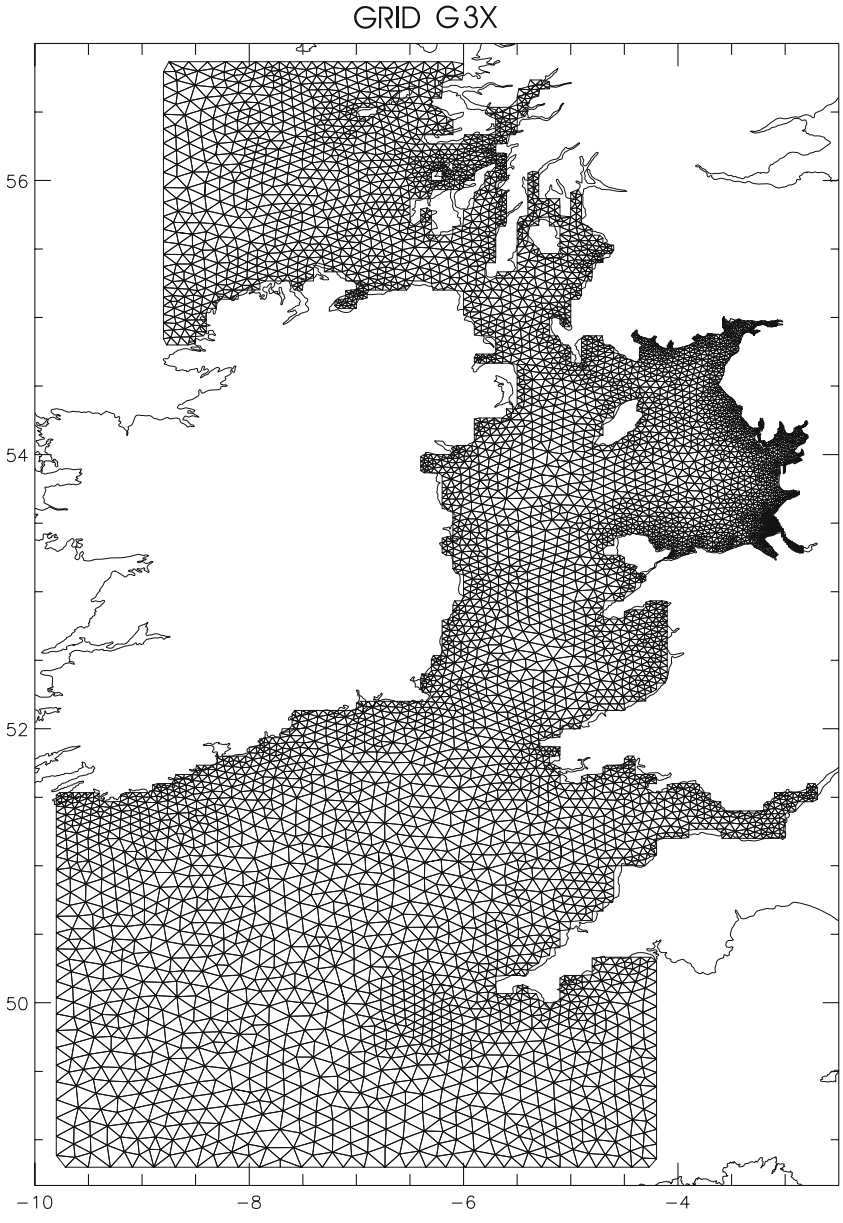


**Fig. 10** The irregular finite element grid (G3X) with non-zero coastal water depths used in Calc.9

tion in $\bar{H}_{EX}$ and RMS errors also occurred. For elevations the number of points within $\pm 10$ cm increases from 73 locations (Calc 9) to 81 locations (Calc 10), although in terms of phase there is no improvement. This suggests that the higher order element slightly improves the accuracy of the solution. Although the increase in accuracy is small, so is the additional computational effort, which suggests that there are benefits in using higher order elements.

## Concluding remarks

A detailed comparison of a finite element model with a range of mesh refinements and an existing coarse grid large area model of the Irish and Celtic Sea regions has been performed. In addition computed tidal elevations over the region have been compared with a comprehensive (214 values) data set of $M_2$ tidal elevation amplitudes and phases. The primary objective of the paper has been to examine how an optimal distribution of elements can be determined to maximize the accuracy of the finite element solution while minimizing the computer time. In parallel with this, the comparison with an existing finite difference model highlights some important differences in determining the choice of computational points to compare with observations. In addition the slight movement of nodes over the whole region as the grid is refined in a specific location adds a degree of complexity that does not occur in the traditional finite difference model.

Although the use of a zero water depth at land, gives a very fine mesh in the coastal region when a water depth related criterion is used in mesh generation, the accuracy

of the solution is reduced compared to specifying a coastal water depth. In addition the computational cost of the calculation is significantly larger. Calculations using a specified water depth at the shoreline, the approach used in the traditional finite difference approach yielded the most accurate solution at a reduced computational effort. This was related to the reduced number of nodes, the smaller number of iterations required at each time step, and the fact that 'wetting and drying' only occurred in a limited number of regions. Solutions at offshore tide gauges were not significantly affected by the choice of nearshore water depths, or coastal grid refinements. However, the energy flux into the eastern Irish Sea and hence tidal amplitudes in this region were influenced by the energy flux through the North Channel. This energy flux was sensitive to resolution in the North Channel.

Although the main objective of the paper was 'like with like' comparison with the 7 km finite difference model, it was clear that solutions in the eastern Irish Sea, Mersey and Bristol Channel were improved when better topography was included in these areas. Improving the local topography in one region, with a depth dependant criterion for mesh generation, caused changes in the location of nodes elsewhere. Since to be consistent with previous finite difference calculations, the comparison criterion was to take the offshore node nearest to the observation point, this meant that as this node changed its location in shallow water, then the depth changed. This had the effect of changing the comparison with observations due to a local change in node position and global change in tide. This change in node position and hence comparison point does not occur in a finite difference model when the 'far field' grid is refined.

Despite these differences, compared to a finite difference model, in fixing the location of the comparison point in the finite element mesh, it is evident that the most accurate solution was derived with the higher order element and a specified coastal water depth. Obviously a more accurate description of nearshore water depths and coastline than that used here would improve the finite element solution. Calculations and comparisons performed here suggest that the exact choice of water depth at the coast and in the near coastal area are crucial in determining the model's accuracy in the coastal region. Water depths in this region together with the degree of 'wetting and drying' and how this is implemented (Flather and Hubbert 1989) determines the energy loss from the $M_2$ tide and the generation of higher harmonics. To progress farther, additional tidal constituents and three-dimensional effects need to be added.

In terms of storm surge calculations where the accurate determination of coastal elevations is crucial then the ability of the finite element model to refine the grid locally is a major advantage. This also avoids the problems of open boundary conditions (Davies et al. 2003; Jones and Davies 2004a, b) when fine mesh limited areas are used. Having determined an accurate tidal solution on an irregular grid, the storm surge problem is presently being examined, as is improved resolution in the eastern Irish Sea to complement measurements made as part of a Coastal Observatory Programme (Proctor and Howarth 2003).

**Acknowledgements** The origin of the TELEMAC SYSTEM is EDF-LNHE and is therefore ©EDF-LNHE. The authors are indebted to Dr Alan Cooper for a number of valuable suggestions on the use of TELEMAC. Typing support provided by Mrs L Parry is very much appreciated.

## References

Davies AM, Jones JE (1992) A three-dimensional wind driven circulation model of the Celtic and Irish Seas. Contin Shelf Research 12:159–188

Davies AM, Jones JE (1995) The influence of bottom and internal friction upon tidal currents: Taylor's problem in three-dimensions. Contin Shelf Res 15:1251–1285

Davies AM, Jones JE, Xing J (1997) Review of recent developments in tidal hydrodynamic modelling, I. Spectral models. J Hydraulic Eng 123:278–292

Davies AM, Kwong SCM (2000) Tidal energy fluxes and dissipation on the European continental shelf. J Geophys Res 105:21969–21989

Davies AM, Hall P, Howarth JM, Knight P, Player R (2001a) A detailed comparison of measured and modelled wind driven currents in the North Channel of the Irish Sea. J Geophys Res 106:19683–19713

Davies AM, Hall P, Howarth MJ, Knight P, Player R (2001b) Comparison of observed (HF Radar and ADCP measurements) and computed tides in the North Channel of the Irish Sea. J Phys Oceanogr 31:1764–1785

Davies AM, Hall P (2002) Numerical problems associated with coupling models in shelf edge regions. Appl Math Model 26:807–831

Davies AM, Xing J (2003) The influence of wind direction upon flow along the west coast of Britain and in the North Channel of the Irish Sea. J Phys Oceanogr 33:57–74

Davies AM, Xing J, Gjevik B (2003) Barotropic eddy generation by flow instability at the shelf edge: sensitivity to open boundary conditions, inflow and diffusion. J Geophys Res 108(C2). doi:10.1029/2001 JC 001137

Flather RA, Hubbert KP (1989) Tide and surge models for shallow water—Morecambe Bay revisited. In: Modeling Marine Systems, vol 1. CRC, Boca Raton, pp 135–166

Flather RA, Smith J (1993) Recent progress with storm surge models—results from January and February 1993. In: Proceedings of the MAFF conference of River and Coastal Engineers, University of Loughborough, pp 6.2.1–6.2.16

Fortunato AB, Baptista AM, Luettich RA (1997) A three-dimensional model of tidal currents in the mouth of the Tagus estuary. Contin Shelf Res 17:1689–1714

Fortunato AB, Oliviera A, Baptists AM (1999) On the effect of tidal flats on the hydrodynamics of the Tagus estuary. Oceanologica Acta 22:31–44

George KJ (1980) Anatomy of an amphidrome. Hydrogr J 18:5–12

Heaps NS (1983) Storm surges, 1967–1982. Geophys J R Astron Soc 74:331–376

Heaps NS, Jones JE (1979) Recent storm surges in the Irish Sea. In: Nihoul JCJ (ed) Marine forecasting. Proceedings of the 10th international Liege colloquium on ocean hydrodynamics, 1978. Elsevier, Amsterdam 493 pp, pp 285–319

Heniche M, Secretin Y, Boudreau P, Leclerc M (2000) A two-dimensional finite element drying-wetting shallow water model for rivers and estuaries. Adv Water Resources 23:359–372

Hervouet J-M (2002) TELEMAC modelling system: an overview. Hydrol Processes 14:2209–2210

Howarth MJ (1990) Atlas of tidal elevations and currents around the British Isles. Department of Energy, Offshore Technology Report OTH 89–293 HMSO, London

Jones JE (1983) Charts of the $O_1$, $K_1$, $N_2$, $M_2$ and $S_2$ tides in the Celtic Sea including $M_2$ and $S_2$ tidal currents. Institute of Oceanographic Sciences, report no. 169, 55pp

Jones JE, Davies AM (1996) A high resolution three-dimensional model of the $M_2$, $M_4$, $M_6$, $S_2$, $N_2$, $K_1$, and $O_1$ tides in the eastern Irish Sea. Estuarine Coastal Shelf Sci 42:311–346

Jones JE, Davies AM (1998) Storm surge computations for the Irish Sea using a three-dimensional numerical model including wave-current interaction. Contin Shelf Res 18:201–251

Jones JE, Davies AM (2001) Influence of wave-current interaction and high frequency forcing upon storm induced currents and elevations. Estuarine Coastal Shelf Sci 53:397–414

Jones JE (2002) Coastal and shelf-sea modelling in the European context. Oceanogr Mar Biol Annu Rev 40:37–141

Jones JE, Davies AM (2003a) Processes influencing storm induced currents in the Irish Sea. J Phys Oceanogr 33:88–104

Jones JE, Davies AM (2003b) On combining current observations and models to investigate the wind induced circulation of the eastern Irish Sea. Contin Shelf Res 23:415–434

Jones JE, Davies AM (2004a) Influence of wind field and open boundary input upon computed negative surges in the Irish Sea. Contin Shelf Res 24:2045–2064

Jones JE, Davies AM (2004b) On the sensitivity of computed surges to open boundary formulation. Ocean Dynam 54:142–162

Knight P, Howarth MJ (1999) The flow through the North Channel of the Irish Sea. Contin Shelf Res 19:693–716

Lennon GW (1963) The identification of weather conditions associated with the generation of major storm surges along the west coast of the British Isles. Q J Res Meteorol Soc 89:381–394

Luettich RA, Westerink JJ (1995) Continental shelf scale convergence studies with a barotropic tidal model. In: Lynch DR, Davies AM (ed) Quantitative skill assessment for Coastal Ocean Models. published American Geophysical Union, pp 349–371

Malcherek A (2000) Application of TELEMAC-2D in a narrow estuarine tributary. Hydrol Processes 14:2293–2300

Proctor R, Howarth MJ (2003) The POL coastal observatory. In 'Building the European Capacity in Operational Oceanography', Proceedings of 3rd international conference on EuroGOOS, 3–6 December 2002, Athens, Greece. Elsevier Oceanography Series, 69:548–553, 698 pp

Robinson IS (1979) The tidal dynamics of the Irish and Celtic Seas. Geophys J R Astron Soc 56:159–197

Werner FE (1995) A field test case for tidally forced flows: a review of the tidal flow forum. In: Lynch DR, Davies AM (eds) Quantitative Skill Assessment for Coastal Ocean Models. Published American Geophysical Union, pp 269–284

Young EF, Aldridge JN, Brown J (2000) Development and validation of a three-dimensional curvilinear model for the study of fluxes through the North Channel of the Irish Sea. Contin Shelf Res 20:997–1035

Young EF, Brown J, Aldridge JN (2001) Application of a large area curvilinear model to the study of the wind-forced dynamics of flows through the North Channel of the Irish Sea. Contin Shelf Res 21:1403–1434